



Norwegian University of
Science and Technology

A Temperature-dependent Model of Ratio of Specific Heats Applying in Diesel Engine

shangming Li

Marine Technology

Submission date: June 2017

Supervisor: Sergey Ushakov, IMT

Norwegian University of Science and Technology
Department of Marine Technology

Abstract

Rate of heat release is a standard tool when engineers tune and develop new engines. The ratio of specific heats γ is considered an essential parameter for achieving accurate rate of heat release calculation as it couples the engine system energy and other thermodynamic properties. The γ model is a function of various factors, such as temperature, air-fuel-ratio, pressure, etc. To improve the accuracy of ROHR calculation in the Scania diesel engine in NTNU machinery laboratory since constant-value γ model is applied there, three existing temperature-dependent γ models are investigated in this work. Some other more complex models considering other factors are not discussed here as real-time computation is required. An engine experiment comprising of constant speed and propeller curve test cycle is carried out for supplying the raw data.

A reference model based on the theory of Zacharias's formulas is established to evaluate the accuracy of three candidate models. The models are evaluated in both γ domain and ROHR domain. Three evaluating criteria including MRE, RMSE and NRMSE are carried out to evaluate the error of models. A retrofit γ model is proposed by applying γ offset value to further improve accuracy in the end.

Preface

Firstly, I would like to send my sincere gratefulness to my supervisor Professor Sergey Ushakov for providing me guidance through this project work and sparing his hours of time reading through my report and giving comments. This feedback is very precious and useful for my thesis.

Nicolas Lefebvre also gives me a lot of advice and inspiration when starting my thesis work.

Kevin Koosup Yum from Marintek helped me a lot with building reference model and gives me much more constructive advice than I expected.

I also want to thank Frode Gran for providing generous guidance in Marine engine laboratory. My friend Jialin Yu also gave me lots of help in MATLAB.

Lastly, I want to express my deepest gratitude to my parents for their support and love.

Table of Contents

| | |
|---|-------------|
| Summary | i |
| Preface | ii |
| Table of Contents | v |
| List of Tables | viii |
| List of Figures | xi |
| Abbreviations | xii |
| 1 Introduction | 1 |
| 1.1 Background | 1 |
| 1.2 Objective | 2 |
| 1.3 Outlines | 3 |
| 2 Theoretic Fundamentals | 5 |
| 2.1 Engine geometry and power strokes | 5 |
| 2.2 Combustion Process | 7 |
| 2.3 Computation of ROHR | 9 |

| | | |
|----------|--|-----------|
| 2.3.1 | Methods | 9 |
| 2.3.2 | In-cylinder Pressure Measurement | 15 |
| 2.3.3 | Cylinder Volume Model | 18 |
| 2.3.4 | Ratio of specific heats models | 19 |
| 2.3.5 | Temperature Model | 24 |
| 2.3.6 | Summary of ROHR Computation components | 25 |
| 3 | Equipments and Test Initialization | 27 |
| 3.1 | Experiment Equipments | 27 |
| 3.1.1 | Engine | 27 |
| 3.1.2 | Pressure Sensor | 28 |
| 3.1.3 | Engine Control Computers | 30 |
| 3.1.4 | Test Fuel | 31 |
| 3.2 | Test Cycle | 32 |
| 3.3 | Perform Test | 33 |
| 4 | Results and Analysis | 35 |
| 4.1 | Results From Raw Test Data | 35 |
| 4.1.1 | In-cylinder pressure | 35 |
| 4.1.2 | ROHR (applying constant γ model) | 37 |
| 4.1.3 | Estimating Temperature Model | 38 |
| 4.1.4 | Existing Temperature-dependent γ Models | 40 |
| 4.2 | Reference Model | 40 |
| 4.2.1 | Basic theory | 40 |
| 4.2.2 | Integrating parameter initialization | 44 |
| 4.2.3 | Iterating process | 46 |
| 4.2.4 | Results demonstration | 47 |
| 4.3 | Model Evaluation | 50 |
| 4.3.1 | Evaluation criteria | 50 |
| 4.3.2 | Results analysis | 51 |

| | | |
|----------|---------------------------------------|-----------|
| 4.4 | A Retrofit γ Model | 54 |
| 4.4.1 | Results evaluation | 56 |
| 5 | Conclusion | 63 |
| 5.1 | Model candidates evaluation | 63 |
| 5.2 | Retrofit model | 64 |
| 5.3 | Future work | 64 |
| | Bibliography | 65 |
| A | Plot of results | 67 |
| B | Zacharias formulas | 81 |
| B.1 | title in toc | 82 |

List of Tables

| | | |
|-----|--|----|
| 2.1 | Parameters summary | 25 |
| 3.1 | Scania engine specification (from engine manufactures) | 28 |
| 3.2 | Technical data of pressure sensor- kistler 6055Bsp | 30 |
| 3.3 | Diesel fuel properties (from EN590) | 31 |
| 3.4 | E2 cycle test points | 32 |
| 3.5 | E3 cycle test points | 32 |
| 4.1 | Input parameters of the subroutine based on theory of Zacharias formulas | 43 |
| 4.2 | Output parameters of the subroutine based on theory of Zacharias formulas | 43 |
| 4.3 | Initial condition data for integration of ordinary differential equations . . | 45 |
| 4.4 | Maximum relative error(MRE) of three γ model candidates at all test points | 51 |
| 4.5 | Normalized root mean square error (NRMSE) of three γ model candidates compared with reference model at all test points | 53 |
| 4.6 | Root mean square error (RMSE) of ROHR computed by three γ model candidates compared with one computed by reference model | 55 |
| 4.7 | Mean error of three γ model candidates comparing to reference model . . | 56 |
| 4.8 | Mean value of MRE among all test points between original γ model can- didates and retrofit model candidates | 58 |

| | | |
|------|---|----|
| 4.9 | Normalized root mean square error(NRMSE) between original γ model candidates and retrofit model candidates | 58 |
| 4.10 | comparison of Root mean square error(RMSE) of ROHR between one computed by constant-value γ model and computed by retrofitted Gatowski's model | 60 |

List of Figures

| | | |
|------|--|----|
| 2.1 | Basic geometry of cylinder [Heywood (1988)] | 6 |
| 2.2 | Four combustion phases in diesel engine [Zhen et al. (2013)] | 7 |
| 2.3 | Close system[Engineering (2013)] | 9 |
| 2.4 | Open system[Engineering (2013)] | 11 |
| 2.5 | Cylinder pressure measuring system[Bueno et al. (2012)] | 15 |
| 2.6 | The piezoelectric pressure transducer[Bueno et al. (2012)] | 16 |
| 2.7 | Dynamic cylinder pressure curve [Bueno et al. (2012)] | 17 |
| 2.8 | Definition of loss angle [Bueno et al. (2012)] | 17 |
| 2.9 | Typical cylinder geometry [Heywood (1988)] | 18 |
| 2.10 | γ variation as a function of equivalence ratio and temperature [Brunt et al. (1998)] | 21 |
| 2.11 | The results of γ calculated in three methods, curve 1 is the <i>Kappa</i> model, 2 and 3 represents Egnell's model and the linear model, respectively [Egnell (1998)] | 23 |
| 3.1 | Scania Engine DI09-072M | 28 |
| 3.2 | Kistler sensor 6055Bsp | 29 |
| 3.3 | Computer and LabVIEW for controlling engine in Machinery lab | 31 |

| | | |
|------|---|----|
| 3.4 | Test cycle : E2 and E3 | 33 |
| 4.1 | The comparison of raw in-cylinder dynamic pressure measurements at all test points of E2 and E3 cycles | 36 |
| 4.2 | ROHR curves calculated by applying constant γ model in E2 cycle | 37 |
| 4.3 | ROHR curves calculated by applying constant γ model in E3 cycle | 38 |
| 4.4 | The comparison of in-cylinder temperature in E2 and E3 cycles, which is gained from computation of temperature estimate model | 39 |
| 4.5 | Comparison of three existing temperature-dependent γ model candidates (Gatowski's model, Brunt's model and Egnell's model) at E2 and E3 test cycle in dynamic states | 41 |
| 4.6 | Reference model iterating process loop | 46 |
| 4.7 | Comparison of estimate temperature model and reference model @220kW/1800RPM condition | 48 |
| 4.8 | Dynamic fuel-air equivalence ratio model gained from reference model @220kW/1800RPM condition | 48 |
| 4.9 | Comparison of reference γ models during the iterating process @220kW/1800RPM condition, the purple line is considered as at converged state. | 49 |
| 4.10 | Comparison of ROHR computed by original constant-value γ model and reference γ model @220kW/1800RPM condition | 50 |
| 4.11 | Two examples of evaluation of three γ model candidates by comparing with reference model. | 52 |
| 4.12 | Comparison of ROHR applying γ model candidates and reference model @220kW/1800RPM | 54 |
| 4.13 | Two examples of comparison of three retrofit γ models with reference model | 57 |
| 4.14 | Comparison of MRE & NRMSE among all test points between original γ model candidates and retrofit model candidates | 59 |

| | |
|--|----|
| 4.15 Comparison between ROHR computing by constant-value γ model and retrofitted Gatowski' model @220kW/1800RPM condition | 61 |
| A.1 Original γ model candidates comparison in <i>E2</i> cycle | 69 |
| A.2 Original γ model candidates comparison in <i>E3</i> cycle | 71 |
| A.3 Retrofit γ model candidates comparison in <i>E2</i> cycle | 73 |
| A.4 Retrofit γ model candidates comparison in <i>E3</i> cycle | 75 |
| A.5 The comparison of ROHR computed by retrofit γ model and constant-value γ in <i>E2</i> cycle | 77 |
| A.6 The comparison of ROHR computed by retrofit γ model and constant-value γ in <i>E3</i> cycle | 79 |

Abbreviations

| | |
|-------|-------------------------------------|
| CAD | = Crank angle degree |
| hp | = horse power |
| kW | = kilo Watts |
| IMEP | = Indicated Mean Effective Pressure |
| MEP | = Mean Effective Pressure |
| MRE | = Maximum relative error |
| NRMSE | = Normalized root mean square error |
| RMSE | = Root mean square error |
| RPM | = Revolution Per Minute |
| ROHR | = Rate of heat release |
| TDC | = Top dead center |

Introduction

1.1 Background

Internal combustion engine has been used to transforming chemical energy into useful mechanical work in various transportation for a long history. Along as the developing of technology, internal combustion engine also have been through several revolutions. The modern engine has a much better performance in both fields of engine performance and emission control.

The more stringent exhaust emission regulations and stronger competition between engine manufactures have driven development of engine technology forward. More complex engine system and advanced engine technologies rely on more accurate in-cylinder data during tuning and optimizing. When analyzing the internal combustion engine, Rate of heat release (ROHR) has always been an critical parameter for evaluation of compartment fire growth, which is essential for analyzing the engine performance and emission controlling.

The ratio of specific heats (also as known of γ) refer to the ratio of heat capacity at con-

stant pressure(C_P) to heat capacity at constant volume(C_V), is considered as an essential parameter when calculating ROHR

$$\lambda = \frac{C_P}{C_V} \quad (1.1)$$

The ratio of specific heat is used to couples the system energy to other thermodynamic quantities. The working medium, in many cases, is considered as ideal gas, thus the ratio of specific heat is set to constant value for the convenience of calculation. While this is not accurate as specific heat is influenced by various factors like temperature, air fuel ratio, etc. Consequently, a more accurate model of specific heat ratio is desired for calculating accurate ROHR curves. Among factors mentioned above, in-cylinder temperature is considered as the dominant one. In this work, three temperature-dependent γ models are introduced are investigated and evaluated for applying in computation of ROHR.

1.2 Objective

NTNU machinery laboratory offers real-time ROHR computation when performing the engine test. While working medium is considered as ideal gas for the convenience of calculation. Correspondingly, the ratio of specific heat is set to be constant value while computing the ROHR, which leads to inaccurate absolute value of rate of heat release. To improve the computing accuracy, the investigation and evaluation on existing γ models are carried out. A reference model shall built up for evaluating the candidate models. The candidate model which fit better with reference model is going to be implemented in ROHR computation module in laboratory.

1.3 Outlines

In chapter 1, the research background of ROHR computation and models of specific heat ratio are introduced. The main objective of this master thesis work is summarized.

In chapter 2, the fundamental knowledge of internal combustion engine and combustion process are reviewed briefly. Two main methods of ROHR computation and the main components for closed-system method are introduced. The existing γ models are investigated in this chapter.

Chapter 3 introduced the set-up of experiment which supplies the fundamental data for further work. The relevant experiment equipment and parameter initialization are presented in this chapter .

Chapter 4 demonstrates the results from experiment and evaluation of γ models candidate. A reference model based on Zacharias formulas and ordinary differential equations is built up for evaluating γ model candidates, the results from comparison between new ROHR curves and the origin ones are discussed. The influence resulting from different λ models and how significant it is analyzed in this chapter.

In chapter 5, the conclusion and future work are presented.

Theoretic Fundamentals

2.1 Engine geometry and power strokes

In general, internal combustion engine is used to convert the chemical energy contained in fuel into the mechanical power. Firstly, Fuel is injected into the cylinder, in where fuel is ignited by spark or high pressure. Combustion is the process in which the fuel and oxygen reacts to release the thermal energy [Heywood (1988)]. The fuel and air mixture are collectively called working fluids. With large amounts of thermal energy released, the working fluids create a high pressure and temperature in-cylinder environment, which drives the piston moving linearly along the cylinder wall. By certain mechanical components (connecting rods and crank shafts), linear force is transferred into desired rotation force (torque) on the shaft.

The basic geometry of cylinder is shown in 2.1, the diameter of cylinder is called Bore. The minimum cylinder volume is achieved when piston is at TDC and when piston is at BDC, cylinder has maximum volume. Minimum volume is called clearance volume V_c . Difference between Maximum volume and clearance volume is called displacement volume V_d . The ratio of max volume to min volume is called compression ratio r_c [Heywood

(1988)].

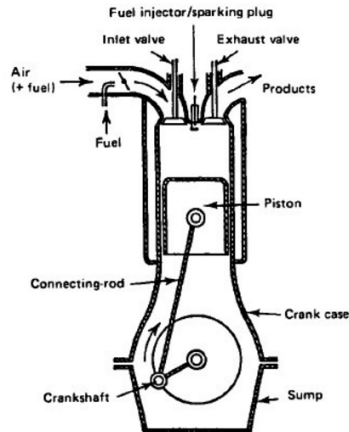


Figure 2.1: Basic geometry of cylinder [Heywood (1988)]

The movement of piston from top position to bottom position or inversely is called a stroke. There are normally two types of internal combustion engine categorized by the number of strokes. Four-stroke engine is mainly used in modern transportation. The reason why four-stroke engine being called four-stroke engine is because it needs four strokes to achieve a power cycle[Heywood (1988)]. One four-stroke cycle comprises:

1. *Intake stroke:* Piston moving from TDC to BDC, fresh mixture enters cylinder. Inlet valve opens before stroke starts and closes when it ends.
2. *Compression stroke:* Piston starts to move upward and compress the cylinder volume. At the end of stroke, ignition starts and pressure rises rapidly.
3. *Power stroke:* Also called as expansion stroke. After combustion starts, working fluids obtain high pressure and temperature and push piston moving downward.
4. *Exhaust stroke:* Exhaust valve opens and piston moves upward to push the exhausted gas out of cylinder.

2.2 Combustion Process

Combustion process in diesel engine can be divided into four phases:

- Ignition delay period
- Premixed combustion phase
- Mixing-controlled combustion phase
- Late combustion phase

All four phases are shown in figure 2.2 below.

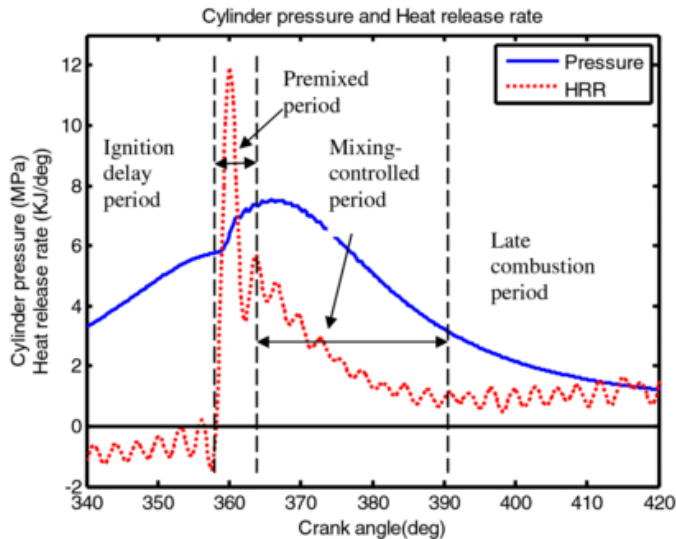


Figure 2.2: Four combustion phases in diesel engine [Zhen et al. (2013)]

Ignition delay period: Unlike spark-ignition engine using sparking plug to ignite, the ignition of diesel fuel results from high temperature caused by high compression ratio of diesel engine. There is an interval between the start of injection and start of combustion [Heywood (1988)], this interval is known as ignition delay.

Ignition delay process can be categorized as physical process and chemical process. The physical process consists of: 1) the atomization of liquid fuel; 2) the vaporization of fuel

droplets; 3) the mixing of fuel vapor and air. The chemical process refers to the pre-combustion reactions of fuel, air, residual gas mixture, which lead to autoignition [Heywood (1988)]. As can be seen from figure 2.2, during ignition delay period, ROHR stays negative value, which may cause by fuel vaporization.

The ignition delay period has essential influence on the further combustion phases: the longer ignition delay is, the more rapidly ROHR will increase in premixed combustion phase. This can lead to high pressure rising rate and high peak pressures. When the ignition occurs late enough to the expansion process for the burning process to be quenched, which results in reduced power output and poor fuel conversion efficiency. In the worst case, it produces audible knocking sound, "diesel knock", which is extremely harmful to engine operation[Heywood (1988)].

Premixed combustion phase:The fuel-air mixture formed in ignition delay period starts to ignite when in-cylinder pressure keeps rising and temperature reaches the auto-ignition point of diesel fuel. A very rapid raise is observed from ROHR curve in figure 2.2. The combustion in this phase is not complete, which leads to produce a large amount of intermediate products(CO and etc.). When homogeneous fuel-air mixture is fully consumed, a steep fall in ROHR curve is discovered. By the end of this phase, diffusion flame is formed.

Mixing-controlled combustion phase: During this phase, diesel fuel keeps injecting into cylinder. The burning rate is more stable and lower as a result of diffusion flame combustion. The stoichiometric fuel-air mixture forms near the flame front, where the thermal energy is released.

Late combustion phase: During the last combustion phase, fuel jet keeps propagating while injection has stopped. The diffusion flame size and mixing rate at flame front are both decreasing. Rate of heat release is degrading correspondingly.

2.3 Computation of ROHR

The rate of heat release gives the important information about the nature of combustion and plays a significant role in the analysis of the engine performance and emissions. However, rate of heat release is not measured directly, it is computed relying on multiple factors. In this section, two main methods used to computed ROHR are presented.

2.3.1 Methods

Close System Approach

The close system method is to assume the whole cylinder volume is a closed system:

- Both inlet and exhaust valves are closed.
- The crevice effect is omitted.
- The enthalpy of injected fuel is neglected.

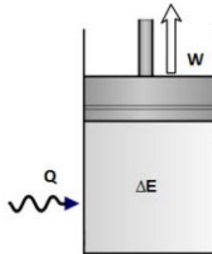


Figure 2.3: Close system[Engineering (2013)]

There is no mass flow across the system boundary. Therefore, the **first law of thermodynamic** applied:[Heywood (1988)]

$$dQ_n = dQ_{ch} - dQ_{ht} = pdV + dU \quad (2.1)$$

where dQ_{ch} is chemical energy of fuel and dQ_{ht} is the heat transfer through cylinder wall. The dQ_n is called apparent net heat-release rate, if further assuming that the working

medium is ideal gas. Then the equation 2.1 becomes:

$$dQ = pdV + mc_v dT \quad (2.2)$$

According to the **ideal gas law**:

$$pv = mRT \quad (2.3)$$

assuming R as constant value, it follows that:

$$\frac{dp}{p} + \frac{dV}{V} = \frac{dT}{T} \quad (2.4)$$

combing equation 2.2 and 2.4, T can be eliminated:

$$dQ_n = \frac{\gamma}{\gamma - 1} pdV + \frac{1}{\gamma - 1} V dp \quad (2.5)$$

Differentiating with respect to the crank angle, the equation used for computing the ROHR is:

$$\frac{dQ_n}{d\phi} = \frac{\gamma}{\gamma - 1} p \frac{dV}{d\phi} + \frac{1}{\gamma - 1} V \frac{dp}{d\phi} \quad (2.6)$$

In summary, this method is based on the assumption that the whole cylinder contents are considered as a closed system. It does not include the effect of leakage and crevices, which actually are parts of the heat release model. Furthermore, the computation is based on the assumption that the gas composition is fixed. However, the aim of using this simplified model is to simplify the computation process. The shape of ROHR curve from close system method remain similar to 'real process' and will be a suitable indicator on combustion process. The more accurate system is to apply open-system model, which is discussed in following section.

Open System Approach

In this method, the cylinder contents are considered as an open system, the mass flow across the system boundary and the varying work medium are taken into the calculation.

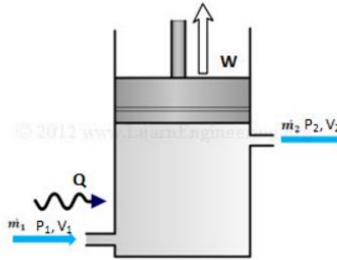


Figure 2.4: Open system[Engineering (2013)]

Some necessary assumptions are made to apply open system analysis:

- Homogeneous working medium
- Instantaneous combustion
- constant rotating speed of crank angle

The **ideal gas law:**

$$pv = mRT \quad (2.7)$$

The R is no longer considered as constant in open system, but a function of pressure P , temperature T and fuel-air equivalence factor F .

$$F = \frac{\frac{m_f}{m_a}}{\left(\frac{m_f}{m_a}\right)_{stoi}} = \frac{f}{f_s} \quad (2.8)$$

Therefore, the equation is differentiated with respect to crank angle:

$$\frac{1}{p} \frac{dp}{d\phi} + \frac{1}{V} \frac{dV}{d\phi} = \frac{1}{m} \frac{dm}{d\phi} + \frac{1}{R} \frac{dR}{d\phi} + \frac{1}{T} \frac{dT}{d\phi} \quad (2.9)$$

Differentiate R with respect to the angle:

$$\frac{dR}{d\phi} = \frac{\partial R}{\partial p} * \frac{dp}{d\phi} + \frac{\partial R}{\partial T} * \frac{dT}{d\phi} + \frac{\partial R}{\partial F} * \frac{dF}{d\phi} \quad (2.10)$$

However, the terms regard to pressure and temperature are normally quite tiny, thus can be neglected in some cases. Combining 2.9 and 2.10, yields the dynamic gas equation:

$$\frac{1}{p} \left[1 - \frac{p}{R} \frac{\partial R}{\partial p} \right] * \frac{dp}{d\phi} - \frac{1}{T} \left[1 + \frac{1}{T} \frac{\partial R}{\partial T} \right] * \frac{dT}{d\phi} - \frac{1}{R} \frac{dR}{dF} * \frac{dF}{d\phi} - \frac{1}{m} \frac{dm}{d\phi} + \frac{1}{V} \frac{dV}{d\phi} = 0 \quad (2.11)$$

This **dynamic gas equation** illustrates the relationship between the gas properties (varying in pressure, temperature and composition) with mass, temperature and pressure.

Energy equation

The energy equation is defined by the first law of thermodynamic. The first law of the thermodynamics for an open system is presented as following:

$$dQ - pdV + \sum_i \dot{m}_i h_i = dU \quad (2.12)$$

where dQ is the heat transfer rate across the system boundary into the system, pdV is the work transfer done by system due to boundary displacement, $\dot{m}_i h_i$ is the enthalpy flux across the system boundary. Possible mass flows dm_i includes: 1) flows in and out the valves; 2) fuel injected directly into the cylinder; 3) flows in and out crevice, etc. U is the internal energy of mass inside the system.

Gas composition

Apart from internal energy, another important component in open system method is the gas composition. The definition of gas composition is described by the equation 2.8, differentiating with respect to the crank angle yields:

$$\frac{dF}{d\phi} = \frac{1}{f_s} * \frac{df}{d\phi} \quad (2.13)$$

$$\frac{df}{d\phi} = \frac{1}{m_A} \left(\frac{dm_F}{d\phi} - f * \frac{dm_A}{d\phi} \right) \quad (2.14)$$

Combining equations 2.13 and 2.14 and rearrange it, the dynamic mixing equation is obtained:

$$\frac{m}{1 + f_s F} * \frac{dF}{d\phi} = \sum_i \frac{F_i - F}{1 + f_s F} * \frac{dm_i}{d\phi} + \frac{1}{f_s} * \frac{dm_f}{d\phi} \quad (2.15)$$

The fuel-air equivalence ratio F is assumed to be zero during compression period. With the fuel injection, F is rising in combustion and keeps constant during the expansion.

The conservation of mass

This section expresses the mass of working medium changing inside the cylinder. The alteration of mass is equal to the mass flow into the system minus the mass flow outside the system, which is described by following equation:

$$\frac{dm}{d\phi} = \frac{dm_i}{d\phi} \quad (2.16)$$

As mentioned in 2.12, m_i includes 1)flows in and out of the valves, 2)fuel injected directly into the cylinder; 3) flows in and out of crevice and etc.

Equations in matrix notation

The matrix which combines four differential equations above is present as following:

$$\begin{bmatrix} \frac{1}{p} \left(1 - \frac{p}{R} \frac{\partial R}{\partial p} \right) & -\frac{1}{T} \left(1 + \frac{T}{R} \frac{\partial R}{\partial T} \right) & -\frac{1}{R} \frac{\partial R}{\partial F} & -\frac{1}{m} \\ m \frac{\partial u}{\partial p} & m \frac{\partial u}{\partial p} & m \frac{\partial u}{\partial p} & u \\ 0 & 0 & \frac{m}{1 + f_s F} & 0 \\ 0 & 0 & 0 & 1 \end{bmatrix} \begin{bmatrix} \frac{dp}{d\phi} \\ \frac{dT}{d\phi} \\ \frac{dF}{d\phi} \\ \frac{dm}{d\phi} \end{bmatrix} = \begin{bmatrix} 0 \\ \frac{dQ}{d\phi} + \sum h * \frac{dm_i}{d\phi} + h_f * \frac{dm_f}{d\phi} \\ \sum_i \frac{F_i - F}{1 + f_s F} * \frac{dm_i}{d\phi} + \frac{1}{f_s} * \frac{dm_f}{d\phi} \\ \sum \frac{dm_i}{d\phi} + \frac{dm_f}{d\phi} \end{bmatrix} \quad (2.17)$$

The state variables and vectors of open system are presented in left, while the interactions

with surroundings are described from right side [Hatlevold (2010)]. The state vectors therefore can be expressed independently by solving this matrix, yields a series of ordinary differential equations. This system of ordinary differential equations can be solved through numerical integration. The integration starts from some points before combustion. Then the ROHR can be computed directly by:

$$ROHR = h_n * \frac{dm_f}{d\phi} \quad (2.18)$$

h_n is net heating value of the fuel. The open system method, which takes real gas properties and heat loss into consideration, is more accurate than close system approach. However, there are some issues increasing the difficulties of applying this approach in diesel engine [Heywood (1988)]:

- The liquid fuel is injected into cylinder and mixing with air. The air-fuel mixture is heterogeneous and varying with time, this process is not quasi static.
- The composition of burned gas is not known
- The correlations for predicting heat transfer in diesel engines is not well defined

Besides, there are some systematic errors existing in both close and open system: 1) *absolute pressure* not known. 2) *Phase shaft between pressure and crank angle*. 3) *Uncertainty* of engine parameter, such as compression ratio. 4) *Truncation*. Limited numerical accuracy of discrete pressure values.

Due to the difficulties and systematic errors existing in the process, both open system and close system method can only obtain approximate output [Heywood (1988)]. In order to implement on LabVIEW for real-time demonstrating, in this master thesis work the close system approach is adopted. The components of close system will be thoroughly discussed in the following section.

2.3.2 In-cylinder Pressure Measurement

The first part introduced for computing the ROHR in close system is dynamic cylinder pressure measurement. Measuring cylinder pressure provides the most reliable information about the dynamic process inside the engine cylinder. A typical method to measure cylinder pressure is using piezoelectric transducer. As can be seen from 2.5, in a typical engine measuring system, a piezoelectric sensor generates a proportional charge towards the pressure change. Therefore, the in-cylinder pressure is obtained by employing a charge amplifier for conditioning the transducer signal. Then the pressure data is sent to PC for storage and further usage.

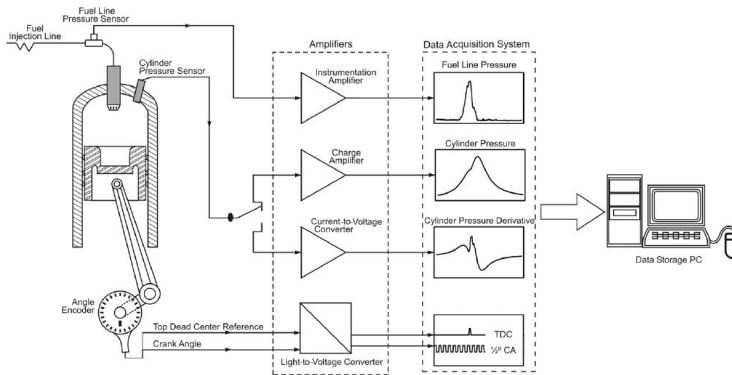


Figure 2.5: Cylinder pressure measuring system[Bueno et al. (2012)]

The figure 2.6 describes the working principle of piezoelectric transducer. The pressure change (dp/dt) results in the deformation changing of piezoelectric crystal element. An electric current therefore is generated due to the piezoelectric effect, which consists of the output signal of sensor:

$$i = -\frac{dq}{dt} = -G_s \frac{dp}{dt} \quad (2.19)$$

Where dq is the deformation polarizes charge, G_s is the transducer sensitivity.

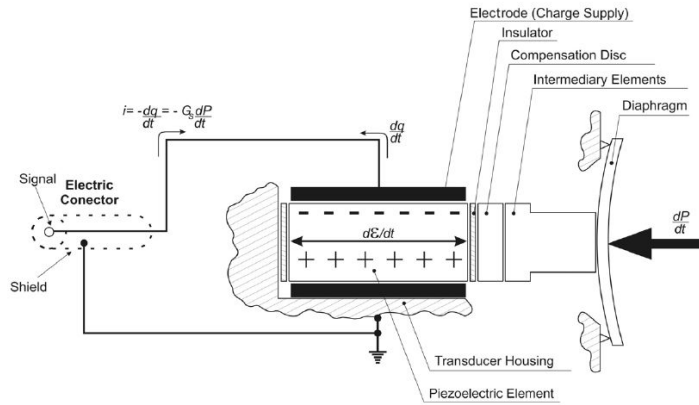


Figure 2.6: The piezoelectric pressure transducer[Bueno et al. (2012)]

Pressure offset

However, the transient heat flow around the sensor continuously changes its temperature. This temperature variation can cause the changing piezoelectric element sensitivity and thermal stress in the sensor housing. The inaccuracy caused by the temperature variation is called temperature drift[Marzouk and Watson (1976)]. When it comes to the heat flow within each cycle, it is named as short-term drift(also called thermal shock). Short-term drift results in higher measurement value than actual cylinder pressure during the combustion, and lower value during the expansion process. To compensate the inaccuracy caused by drift, a pressure sensor model is applied[Klein (2004)]:

$$p_m = K_p * p + \Delta p \quad (2.20)$$

where p_m is measured cylinder pressure and p is the actual cylinder pressure. The gain K_p is determined by measurement setup. The offset Δp varies during a cycle process to compensate effect of short-term drift. The drift, for the convenience of calculation, can be assumed to be very slow, the Δp thus can be set as constant value [Klein (2004)]. The pressure offset can be estimated by various methods: 1) Find Δp in a least square sense using a polytropic model in cylinder pressure p . 2) Sampling intake manifold pressure

p_{man} for several times as the reference pressure to measured cylinder pressure p_m [Klein (2004)]. According the information given by sensor manufacturer, Δp is set to 0.5 bar and K_p as 1.

Crank angle phasing

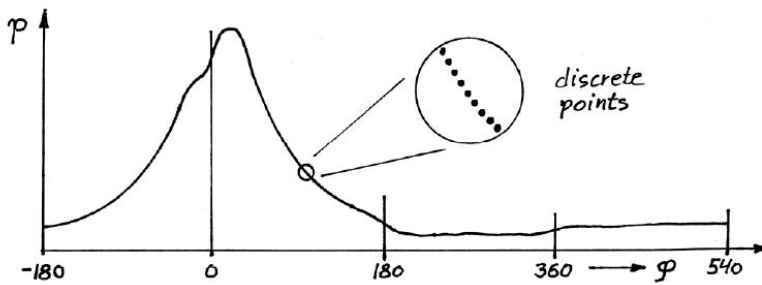


Figure 2.7: Dynamic cylinder pressure curve [Bueno et al. (2012)]

The cylinder pressure curve is sampled as discrete points, as can be observed from figure 2.7. These discrete points response to the different crank angle. To measure the crank angle, TDC position is normally used as a reference position. The TDC position identification is inferred by cylinder pressure data. In fact, the peak pressure precedes actual TDC position, which is shown in figure 2.8.

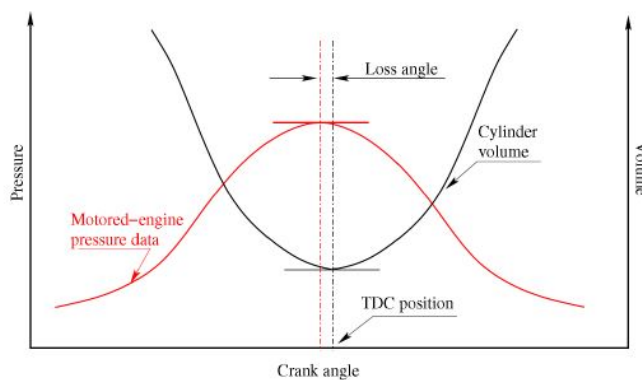


Figure 2.8: Definition of loss angle [Bueno et al. (2012)]

This loss angle can result in the inaccuracy of crank angle phasing. Therefore, the phasing of pressure trace relative to the volume trace will definitely have impact on the ROHR calculating. To minimize this inaccuracy, a constant offset θ_0 is added to the crank angle model:

$$\theta_i + \theta_o = \theta_{i,ture} \quad (2.21)$$

where θ_i and $\theta_{i,ture}$ are measured and real crank angle, respectively. θ_0 in this experiment is set to 0.5° .

2.3.3 Cylinder Volume Model

Cylinder volume is another important component in ROHR computation model. Unlike dynamic cylinder pressure is measured, the cylinder volume function is determined by the geometry of engine cylinder, which is fixed since it was produced from manufacturers. The typical geometry of cylinder is presented in figure 2.9:

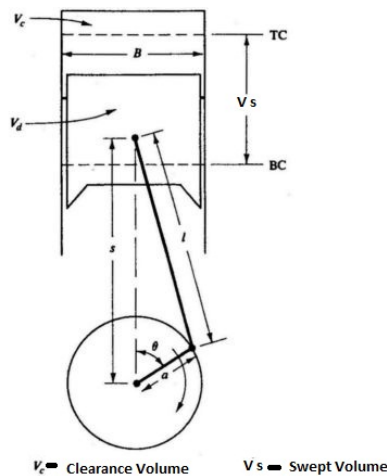


Figure 2.9: Typical cylinder geometry [Heywood (1988)]

The cylinder volume $V(\phi)$ consists of two parts: a clearance volume V_c and an instantaneous displacement volume $V_{id}(\phi)$, presenting as following:

$$V(\phi) = V_c + V_{id}(\phi) \quad (2.22)$$

Meanwhile, based on the geometry of engine cylinder, the $V_{id}(\phi)$ can be derived as :

$$V_{id}(\phi) = \frac{V_d}{2} [1 - \cos\phi + (1/\lambda)(1 - \sqrt{1 - (\lambda\sin\phi)^2})] \quad (2.23)$$

where V_d is the fixed displacement volume of cylinder, can be determined by the other engine parameters(such as bore and stroke). λ is the crank ratio, crank radius divided by connecting rod length. To combine equation 2.22 and 2.23, the final equation is obtained as:

$$V(\phi) = V_c + \frac{V_d}{2} [1 - \cos\phi + (1/\lambda)(1 - \sqrt{1 - (\lambda\sin\phi)^2})] \quad (2.24)$$

For the convenience of computing ROHR, here dynamic cylinder volume is differentiated with respect of crank angle :

$$\frac{dV}{d\phi} = \frac{v_d}{2} \left[\sin\phi + \frac{\lambda\sin 2\phi}{2\sqrt{1 - (\lambda\sin\phi)^2}} \right] \quad (2.25)$$

2.3.4 Ratio of specific heats models

The most important thermodynamic property used in calculating the ROHR is the ratio of specific heats (also known as γ) [Chun and Heywood (1987)]. In many cases, the γ is assumed as constant value for the convenience of calculation. However, as all known, the γ is function of various factors such as temperature, pressure, air-fuel ratio, etc. Therefore, it is inaccurate to compute ROHR with constant value γ model. Among these factors affecting γ , the charge temperature is considered as the most important one. In this section, three existing models of *ratio of specific heat* are introduced: 1) a simple linear model in temperature used in Gatowski et al. (1984). 2) a more complex model from [Brunt et al. (1998)] with higher order function of temperature. 3) the exponential model proposed by [Egnell (1998)]. These three existing γ models are called γ model candidates in the

following chapters and will be evaluated by experiment data and a reference model.

Linear model in T (Gatowski's model)

In the first proposed model, the ratio of specific heats is only the function of temperature. According to [Gatowski et al. (1984)], ratio of specific heats for closed part of cycle is modeled as a linear function of temperature. The linear function in T can be written as following:

$$\gamma_{lin}(T) = \gamma_{300} + b(T - 300) \quad (2.26)$$

where γ_{300} is the ratio of specific heats at temperature 300K and b is the slope of this linear function. These two parameters, which determine the model of γ , have to be adjusted by the temperature region and air fuel ratio λ the model will be through. Two proposals are included in [Gatowski et al. (1984)]: one was used for analysis of engine operated in stoichiometric mixture while the other was used for leaner fuel-air mixture. In this work, diesel engine normally operates at lean mixture environment, thus equation [2.27] is applied further for representing linear temperature-dependent γ model.

$$\gamma_{lin}(T) = 1.375 - 6.99 * 10^{(-5)} * T \quad (2.27)$$

This model can be also modified to second or higher order polynomial function of T which is described in the next section.

Higher order polynomial model in T (Brunt's model)

A higher order polynomial model of γ has been presented by [Brunt et al. (1998)]. By applying this higher order model, there is no necessity to set different values of γ_{300} and b for different temperature region and air fuel ratio. The ratio of specific heats γ is known to be a function of charge temperature and composition(including AFR,EGR, fuel properties and ratio of reactants and combustion products). According to [Brunt et al. (1998)], the

difference of γ caused by charged composition is tiny, thus the second order model in charge temperature should be adequate for a particular fuel.

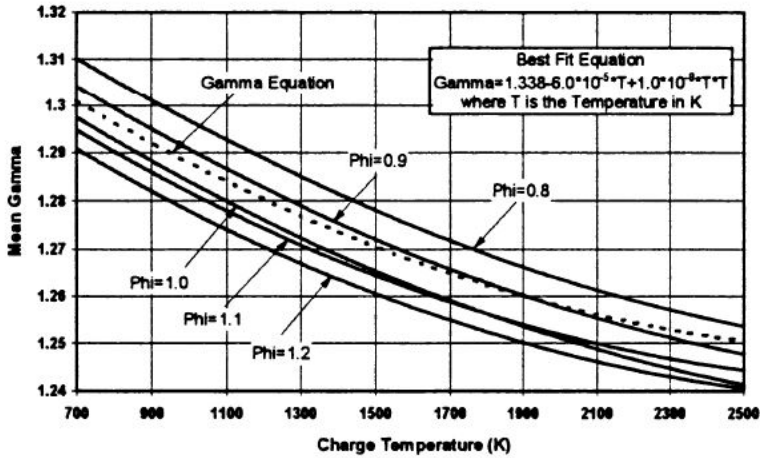


Figure 2.10: γ variation as a function of equivalence ratio and temperature [Brunt et al. (1998)]

The figure 2.10 shows how γ varies as a function of overall equivalence ratio and charge temperature. As can be observed, the variation of γ with equivalence ratio is significant but still much weaker than the impact of temperature. Therefore, a second order correlation between γ and temperature is achieved by finding a reasonable fit from large amounts of data [Brunt et al. (1998)]:

$$\gamma = 1.338 - 6.0 * 10^{-5} * T + 1.0 * 10^{-8} * T^2 \quad (2.28)$$

where T is the charge temperature in K. This correlation is accurate when the air-fuel equivalence ratio is within the range of 0.8 to 1.2: the significance of ignoring the impact of equivalence ratio is an error of up to ± 0.015 in γ , which can cause maximum 0.01 of error in calculating rate of heat release.

Exponential function in T (Egnell's model)

The last model is proposed by Egnell in 1998. The model is an exponential function of temperature, which is presented as:

$$\gamma = \gamma_0 - k_1 \exp(-k_2/T) \quad (2.29)$$

where the parameters are set as:

$$\gamma_0 = 1.38$$

$$k_1 = 0.2$$

$$k_2 = 900$$

To investigate this model, Egnell set two reference models for the results comparison:

1)

$$\gamma = Kappa(GAS, T) \quad (2.30)$$

where *Kappa* in model 1) is a MATLAB function which can compute the γ based on using a vector GAS for a given mixture of gases and charge temperature. This model is highly accurate because GAS vector contains the different gas properties for unburned mixture and combustion products. To be specific, the air-fuel equivalence ratio (λ) of unburned mixture is set with 1, 1.25, 1.5 and 2.0, respectively. While the products of combustion are assumed owning a constant value of λ as 1 [Egnell (1998)].

2)

$$\lambda = \lambda_0 - K_1(T - T_{ref})/1000 \quad (2.31)$$

where λ_0 , K_1 and T_{ref} are 1.38, 0.08 and 300, respectively. This model is the same as the linear model given by [Gatowski et al. (1984)].

The comparison between three methods of calculation is observed in 2.11, Egnell's model fits well with *Kappa* model over entire temperature range, while Gatowski's linear model could only give a good fit in very narrow temperature range.

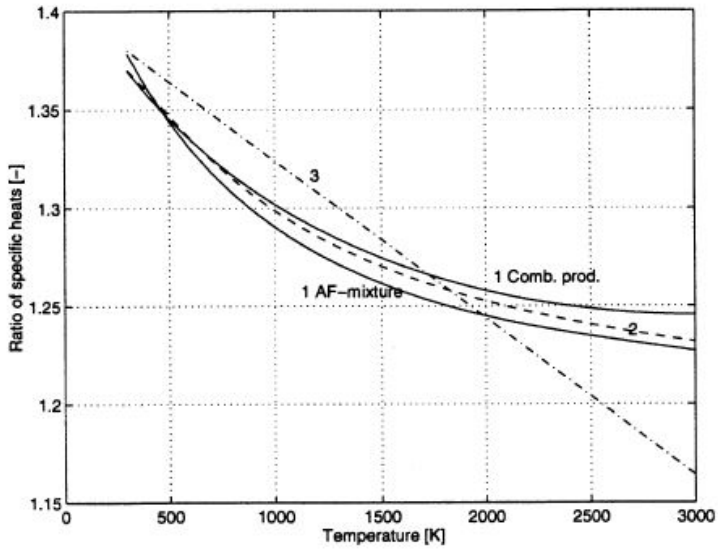


Figure 2.11: The results of γ calculated in three methods, curve 1 is the *Kappa* model, 2 and 3 represents Egnell's model and the linear model, respectively [Egnell (1998)]

Summary of existing models

Three temperature-dependent γ model candidates are introduced in this section, including:

- a simple linear model given by Gatowski et al. (1984):

$$\gamma_{lin}(T) = 1.375 - 6.99 * 10^{-5} * T \quad (2.32)$$

- a higher order polynomial model proposed by Brunt et al. (1998):

$$\gamma = 1.338 - 6.0 * 10^{-5} * T + 1.0 * 10^{-8} * T^2 \quad (2.33)$$

- an exponential model presented by Egnell (1998):

$$\gamma = 1.38 - 0.2 * \exp(-900/T) \quad (2.34)$$

As a matter of fact, γ model does not only vary with the temperature, it is also a function of charge composition, in terms of air-fuel ratio, fuel specification and ratio of reactants to combustion products. For instance, Krieger and Borman proposed a more complex polynomial model in 1967 that took pressure, temperature and air-fuel ratio as variables. While generally, difference caused by charge composition at the same temperature is relatively small, therefore simple equations relating γ to temperature are adequate for a particular fuel [Brunt et al. (1998)]. In addition, to provide real-time ROHR computation in laboratory, the simplicity of model must be considered.

2.3.5 Temperature Model

The in-cylinder temperature is an essential variable because all three λ models proposed above are temperature-dependent model. In this section, an in-cylinder temperature model which was used in [Gatowski et al. (1984)] to estimate mean charge temperature is introduced. The basic equation for computing the mean charge temperature is equation of state:

$$pV = m_c RT$$

according to Gatowski et al. (1984), the molecular weight of reactants and products are essentially the same, the total mass of charge m_c and gas constant R therefore are assumed to be constant. To computed dynamic in-cylinder temperature T , a reference condition, including pressure, temperature and cylinder volume, is required consequently. The equation for determining the charge temperature is:

$$T = \frac{T_{ref}}{p_{ref} V_{ref}} pV \quad (2.35)$$

where T_{ref} , P_{ref} , V_{ref} are the thermodynamic states at the time of reference state. V_{ref} is given by the calculation from equation 2.24. P_{ref} data, varying with different load/RPM conditions, is achieved from in-cylinder pressure measurement. According to the information on a similar engine given by laboratory, the reference position is set at 180° (the end

of inlet-stroke), the mean charge temperature at reference position T_{ref} is set to 315K.

2.3.6 Summary of ROHR Computation components

ROHR computing equation (close system) (2.6):

$$\frac{dQ_n}{d\phi} = \frac{\gamma}{\gamma - 1} p \frac{dV}{d\phi} + \frac{1}{\gamma - 1} V \frac{dp}{d\phi}$$

In-cylinder pressure measuring model (2.20)

$$p_m = K_p * p + \Delta p$$

Crank angle model (2.21):

$$\theta_i + \theta_o = \theta_{i,ture}$$

Cylinder volume differential model (2.25):

$$\frac{dV}{d\phi} = \frac{v_d}{2} \left[\sin\phi + \frac{\lambda \sin 2\phi}{2\sqrt{1 - (\lambda \sin\phi)^2}} \right]$$

In-cylinder temperature estimating model (2.35):

$$T = \frac{T_{ref}}{p_{ref} V_{ref}} pV$$

The nominal values for parameters in close-system method computation of ROHR:

| Parameters | Description | Value | Equation |
|------------|---|---------|----------|
| K_p | pressure model gain | 1 | 2.20 |
| Δp | pressure offset [Bar] | 0.5 | 2.20 |
| θ_o | crank angle offset [degree] | 0.5 | 2.21 |
| T_{ref} | mean charge temperature at reference position [K] | 315 | 2.35 |
| p_{ref} | in-cylinder pressure at reference position [Bar] | depends | 2.35 |
| V_{ref} | cylinder volume at reference position [m^3] | 0.002 | 2.35 |

Table 2.1: Parameters summary

In this chapter, theory background of this master thesis work has been introduced, con-

sisting of ROHR computation methods and components of close system model. Above all, three existing temperature-dependent ratio of specific heats γ models are introduced in sequence. The experiment equipments and test set-up will be demonstrated in next chapter.

Equipments and Test Initialization

This master work is to evaluate three existing temperature-dependent λ models and find a more accurate model for implementing in the ROHR computation module in NTNU Machinery Laboratory. The experiment equipments in the laboratory and test set-up are specified in this chapter.

3.1 Experiment Equipments

In this section, equipments related to the computation of ROHR, consisting of a diesel engine, pressure sensor, Engine control computers and software are introduced in sequence.

3.1.1 Engine

The engine used to test is Scania DI09-072M in Machinery Laboratory. This marine engine is 5-cylinder diesel engine with turbocharger and the nominal power of engine reaches to 221 kW (300hp). The specification data of engine is shown in the table 3.1.

The engine is designed with 4 valves in each cylinder, which promotes the repairability and fuel economy. A eddy-current brake is coupled to the crank shaft of engine in order to

| Engine | Scania DI09-072M |
|------------------------------|--------------------------|
| No. of cylinders | 5 in-line |
| Working principle | 4-stroke |
| Firing order | 1-2-4-5-3 |
| Displacement | 9.3 liters |
| Bore x stroke | 130 x 140 mm |
| Compression ratio | 18:1 |
| Weight (with heat exchanger) | 1150 kg |
| Length of connecting rod | 255mm |
| Max nominal power | 221 kW at 2100 rpm |
| Max brake torque | 1620 Nm at 1100-1300 rpm |

Table 3.1: Scania engine specification (from engine manufactures)

provide loads and measure the torque created by engine. In addition, a bunch of sensors and devices, which can be observed from 3.1 are mounted to measure the various engine performance characters and emissions.



Figure 3.1: Scania Engine DI09-072M

3.1.2 Pressure Sensor

The pressure sensor mounted in Scania engine is Kistler pressure transducer type 6055Bsp, which is belongs to the category of piezoelectric transducer. The working principle of

piezoelectric transducer has been demonstrated in 2.3.2. The sensors is mounted in a specially made transducer adaptor which fits into the heater plug access hole in the cylinder head. 6055Bsp transducer is capable of measuring pressure from 0 to 250 bar in the temperature range between -50 and 350 °C. The front sealing design ensure the efficient heat dissipation, therefore a maximum operating temperature for short-time measuring is 400 °C. The technical data of this transducer is present in 3.2.

There are several certain advantages to use 6055Bsp transducer according to the sensor manufacturer:

- *Knocking resistancy.* The rugged, turned diaphragm allows to measure during the knocking operation.
- *Low thermal shock error* thanks to its front sealing design.
- *High sensitivity:* achieved by utilizing the new piezoelectric crystal

What is worth mentioning, the pressure offset Δp introduced in chapter 2, which is caused by the short-time drift, is given by the manufacturer. According to 3.2, the pressure offset Δp during the dynamic pressure measuring is set to 0.5 bar.

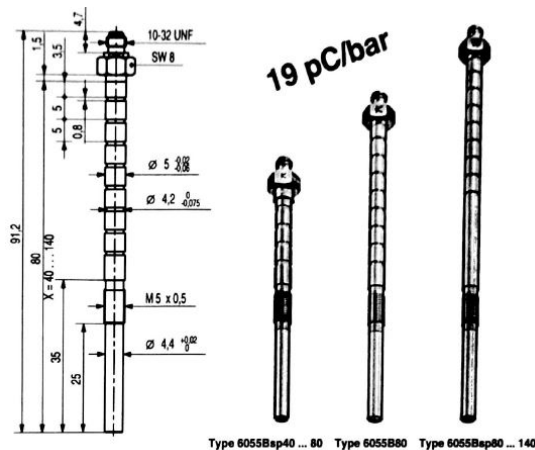


Figure 3.2: Kistler sensor 6055Bsp

| Item | Unit | Value |
|---|------------|-----------|
| Measuring Range | Bar | 0...250 |
| Operating Temperature Range | °C | -50...350 |
| Overload Pressure | Bar | 300 |
| Sensitivity | pC/bar | -19 |
| Natural Frequency | kHz | 130 |
| Linearity | %FSO | <= +/-0.4 |
| Acceleration Sensitivity | Bar/g | <=0.001 |
| Sensitivity shift (200...+/-50°C | % | <=+/-1 |
| Short-time drift error (thermo shock) at 1500r/min, 9 bar IMEP | Bar | <+/-0.5 |
| Insulation resistance | T ω | >=10 |
| Shock Resistanc | g | 2000 |
| Tightening Torque | Nm | 1.5 |
| Capacitance(6055B80) | pF | 25 |
| Weight(6055B80) | g | 10 |
| Plug (teflon insulator) | type | 10-32 UNF |

Table 3.2: Technical data of pressure sensor- kistler 6055Bsp

3.1.3 Engine Control Computers

The Scania engine is controlled by a virtual engineering workbench, LabVIEW. When engine is running, various loading and RPM conditions can be obtained by adjusting the throttle opening and eddy-current brake percentage in LabVIEW interface. Apart from loading and RPM conditions, other static performance data (including torque, IMEP and various emissions) are shown in the main interface of LabVIEW. As can be seen in 3.3, in the left screen, the dynamic data such as in-cylinder pressure, ROHR and accumulated heat release are present instantaneously.

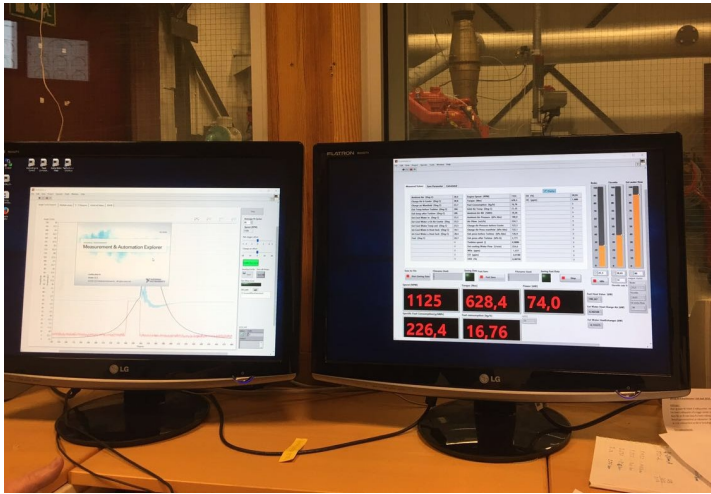


Figure 3.3: Computer and LabVIEW for controlling engine in Machinery lab

3.1.4 Test Fuel

In this test, conventional diesel was used as test fuel. Some basic properties are listed in the table 3.3,

| Properties | Unit | Value |
|---|--------------------|--------|
| Cetane Number | – | 75-80 |
| Density(15°C) | kg/m ³ | 780 |
| Energy content | MJ/kg | 44.1 |
| stoichiometric fuel-air equivalence ratio | – | 0.0683 |
| Polycyclic aromatic hydrocarbons content | % | <0.1 |
| Sulfur content | mg/kg | <0.1 |
| Ash content | mg/kg | 0.001 |
| Water content | mg/kg | 22 |
| Total contamination | mg/kg | <1 |
| Lubricity | | 290 |
| Viscosity | mm ² /s | 2.95 |
| Oxidation stability | g/m ³ | 5 |

Table 3.3: Diesel fuel properties (from EN590)

3.2 Test Cycle

To test the performance of different γ models on different engine operating conditions, two test cycles are chose in this work. E-type test cycle is defined for "Marine application" in the standards of ISO-8178. Cycle E2 is designed for heavy duty constant speed engines for ship propulsion. In E2 cycle, there are 4 points overall, engine speed is set to be constant while power is set to the range from 220kW to 55kW, reduced 55kW each point. For the test cycle E3, which is also known as 'Propeller curve', the power figures are percentage values of the maximum rated power at the rated speed as this cycle is based on a theoretical propeller characteristic curve for vessels driven by heavy duty engines[12]. Four test points are designed in this cycle, power is set to the range from 220kW to 55kW, 55kW less for each point, while the engine speed is set as 1800RPM, 1638RPM, 1440RPM and 1134RPM respectively, not reduced linearly.

| Test point | Power (kW) | ISO-Standard Power (%) | Engine speed (RPM) | ISO-Standard Speed (%) |
|------------|------------|------------------------|--------------------|------------------------|
| 1 | 220 | 100 | 1800 | 100 |
| 2 | 165 | 75 | 1800 | 100 |
| 3 | 110 | 50 | 1800 | 100 |
| 4 | 55 | 25 | 1800 | 100 |

Table 3.4: E2 cycle test points

| Test point | Power (kW) | ISO-Standard Power (%) | Engine speed (RPM) | ISO-Standard Speed (%) |
|------------|------------|------------------------|--------------------|------------------------|
| 1 | 220 | 100 | 1800 | 100 |
| 2 | 165 | 75 | 1638 | 91 |
| 3 | 110 | 50 | 1440 | 80 |
| 4 | 55 | 25 | 1134 | 63 |

Table 3.5: E3 cycle test points

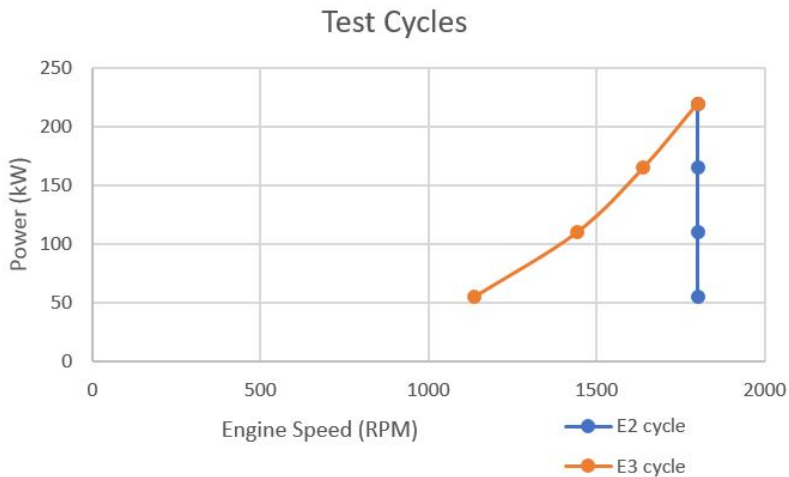


Figure 3.4: Test cycle : E2 and E3

3.3 Perform Test

Before start of tests, the preconditioning work is important to result in better measurements with less uncertainty. It is advised to warm up the engine under load conditions higher than 80% running for over half an hour to stabilize engine parameters. By carrying out warm-up, engine can have better performance. Furthermore, engine calibration work is done at warm condition. Both of two aspects are contributing to yield better measurement quality.

After warm-up, engine is operating at different test points by tuning the percentage of throttle opening and eddy current brake. However, it is not advised to measure immediately. According advice from manufacturer, when switch to a new test point, engine should be left to run at least 15 minutes at that condition to ensure engine performance and emissions are measured at stable condition, where there is less uncertainties affecting.

In next chapter, the results from raw test data (including pressure, temperature, γ and ROHR) and a reference model used to evaluate existing γ models will be introduced.

Results and Analysis

In this chapter, the results are demonstrated and analyzed. Furthermore, to evaluate accuracy of existing γ models, a reference model based on Zacharia's formulas is introduced. The comparison between three existing models and reference model is carried out and results are discussed subsequently. Lastly, model candidates are retrofitted by applying absolute value offset and evaluated again.

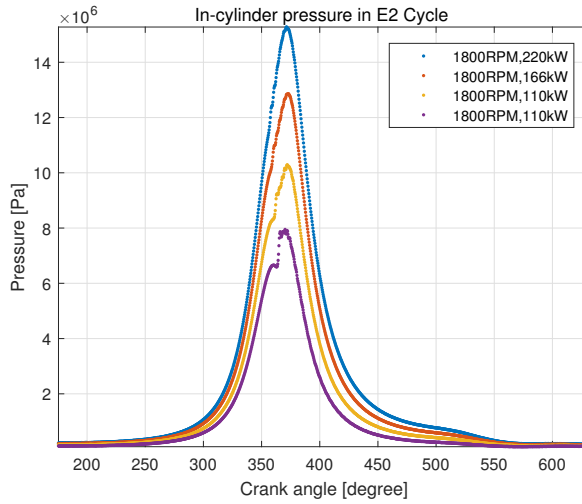
4.1 Results From Raw Test Data

In this section, the results of in-cylinder pressure, ROHR (applying constant γ value), in-cylinder temperature and three temperature- dependent γ models are presented in sequence.

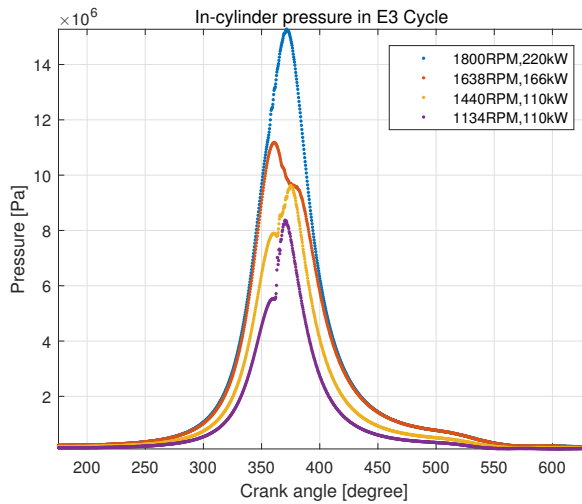
4.1.1 In-cylinder pressure

In-cylinder pressure in this experiment was measured 10 cycles for each test point and pressure sensor sampled 2048 times within each cycle. The results are shown in figure4.1 and as can be easily observed, the higher load conditions yield higher peak pressure for both two cycles. The peak pressure intends to decrease with the drop of Engine speed. In

addition, it is found that peak pressure of four test points in E3 cycle occurred at different crank angles, while in constant-speed cycle all four test points have the highest pressure at roughly same crank angle.



(a) E2 cycle



(b) E3 cycle

Figure 4.1: The comparison of raw in-cylinder dynamic pressure measurements at all test points of E2 and E3 cycles

4.1.2 ROHR (applying constant γ model)

The real-time ROHR computation module of Scania engine applies constant-value γ . In this section, the ROHR curves computed by original method are presented in figure 4.2 and 4.3. Obvious oscillation can be observed on curves as differentiation in computation process, which amplifies the small oscillation in in-cylinder pressure curves. Meanwhile, it is found that the highest value of ROHR decreases with drop of load and engine speed. On the other side, the first spike representing premixed phase combustion gives higher value with lower load and engine speed.

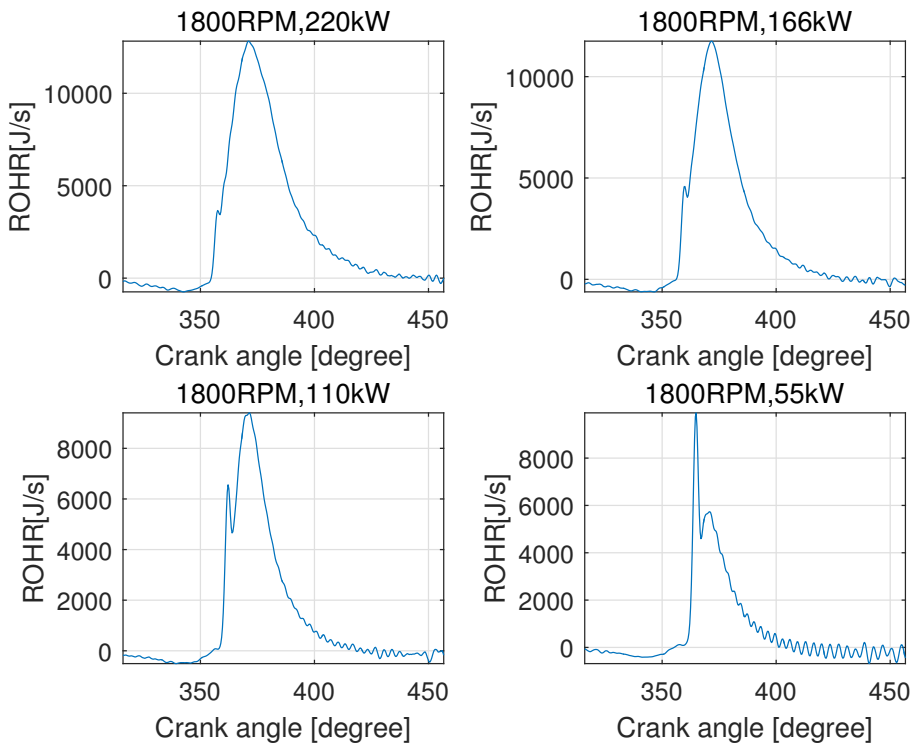


Figure 4.2: ROHR curves calculated by applying constant γ model in E2 cycle

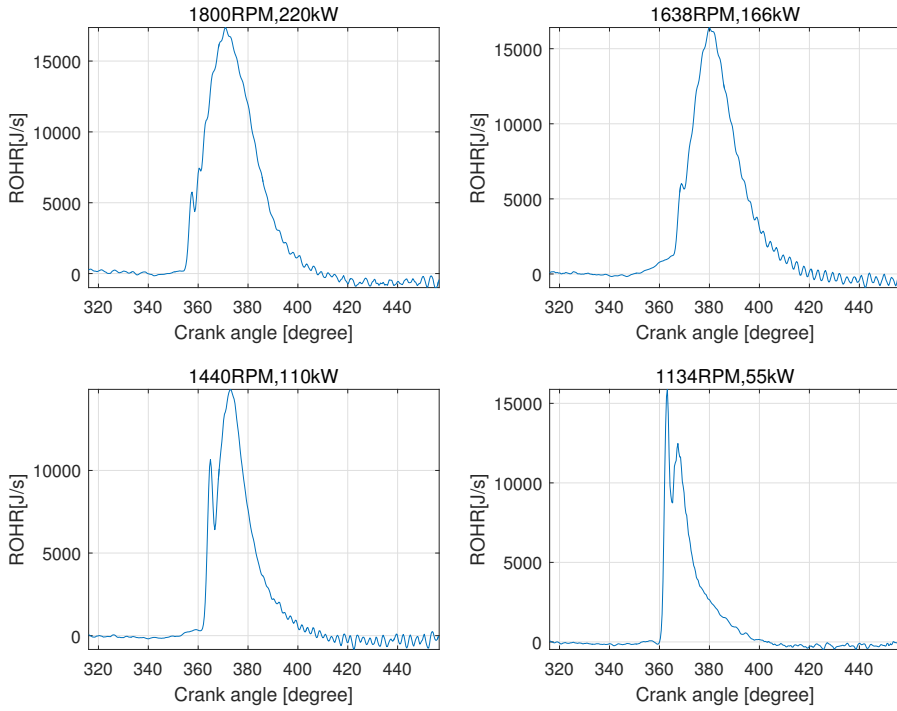


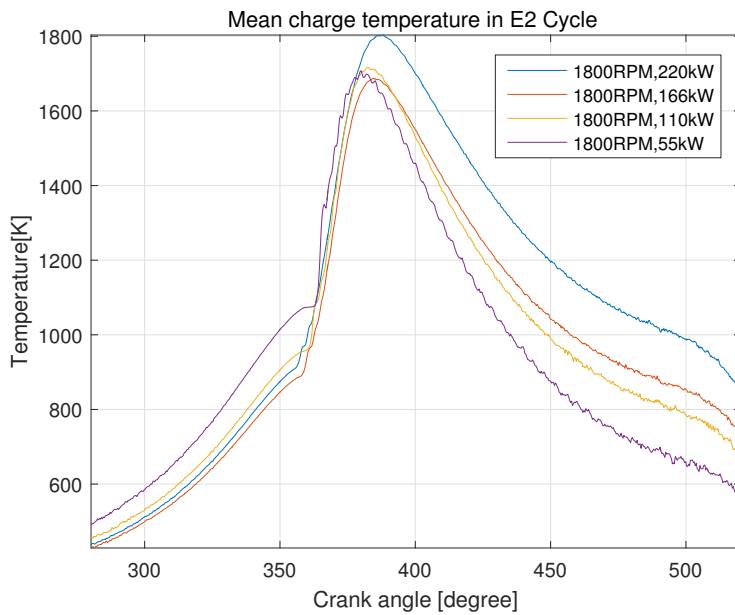
Figure 4.3: ROHR curves calculated by applying constant γ model in E3 cycle

4.1.3 Estimating Temperature Model

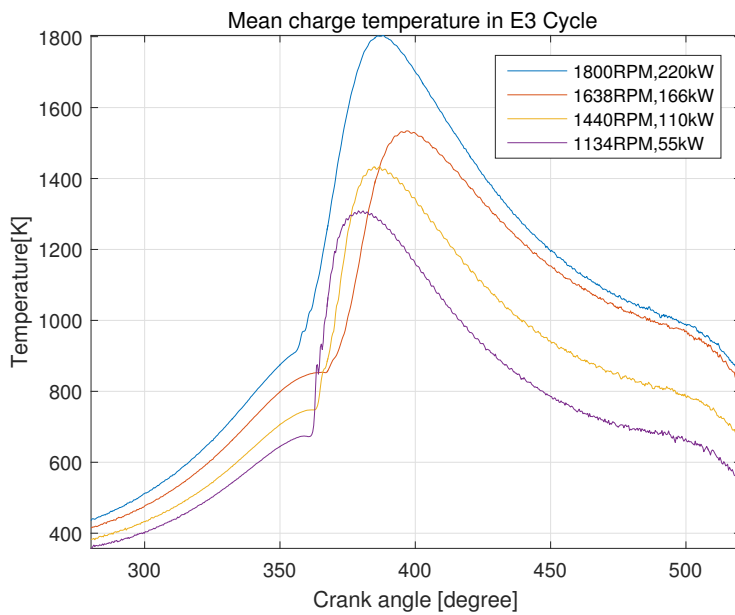
In section 2.3.5, a simplified in-cylinder temperature model used in Gatowski et al. (1984) has been introduced:

$$T = \frac{T_{ref}}{p_{ref} V_{ref}} pV$$

where reference position is at the 180 CAD, T_{ref} is set as 315K, V_{ref} is calculated as $0.002m^3$. The dynamic temperature traces are presented in figure 4.4. As shown, in both cycles the temperature surges rapidly at around TDC position and peak temperature is decreasing when load and engine speed are decreasing.



(a) E2 cycle



(b) E3 cycle

Figure 4.4: The comparison of in-cylinder temperature in E2 and E3 cycles, which is gained from computation of temperature estimate model

4.1.4 Existing Temperature-dependent γ Models

Three existing temperature-dependent γ Models: 1) simple linear model described by equation 2.32 from Gatowski et al. (1984)(Gatowski's model); 2) polynomial model described in equation 2.33 from Brunt et al. (1998) (Brunt's model); 3) exponential model in equation 2.34 from Egnell (1998) (Egnell's model). The in-cylinder dynamic temperature data from figure 4.4 are applied, the results of γ models in two test cycles are shown in figure 4.5. As shown, a phenomenon that all three γ models having lower values during high-temperature zone is observed in both cycles. In addition, Gatowski' model appears to be the most sensitive to in-cylinder temperature: by giving the biggest differential of γ value in different temperature region. On the other hand, Brunt's model is the least sensitive one.

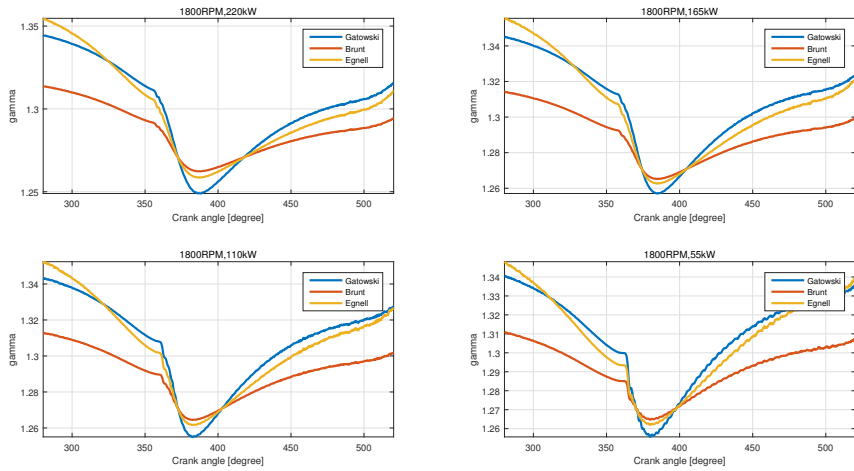
4.2 Reference Model

In the previous chapter, three temperature-dependent γ models have been implemented in MATLAB, and traces of γ within cycles of various operating conditions show the difference. However, it is necessary to distinguish the superiority of model candidates. A more accurate reference model is desired to help select a more suitable γ model for Scania engine. In this section, a reference model based on Zacharias's formulas and open-system ordinary differential equations are built up to evaluate existing models.

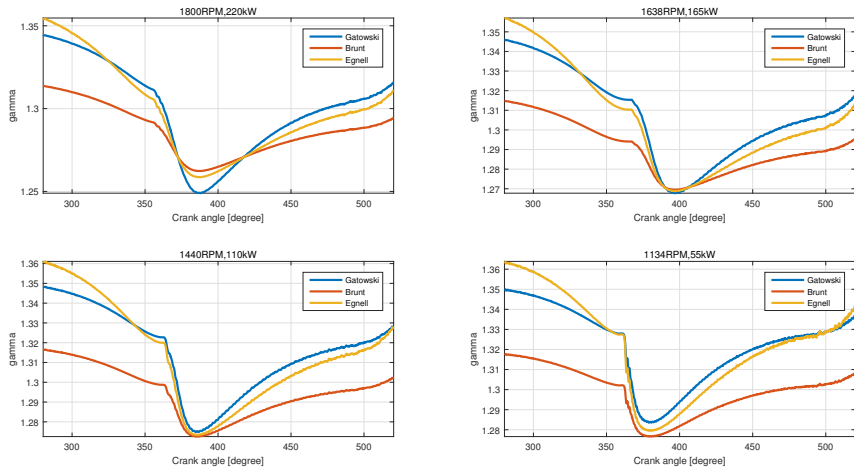
4.2.1 Basic theory

Zacharias formulas

Computation of combustion processes and power cycles require realistic thermodynamic properties of the working medium [Valland (1998)]. F. Zacharias developed formulas for computing thermodynamic properties of combustion products at chemical equilibrium formed by a pure hydrocarbon fuel and dry air. Zacharias computed extensive chemical equilibrium for combustion products together with its thermodynamic properties in a wide



(a) E2 cycle



(b) E3 cycle

Figure 4.5: Comparison of three existing temperature-dependent γ model candidates (Gatowski's model, Brunt's model and Egnell's model) at E2 and E3 test cycle in dynamic states

range of temperature and pressure. Afterwards, a set of three basic functions, known as Zacharias formulas, are obtained by fitting a modified Beattie-Bridgeman type equation of state to his computed database [Valland (1998)]. The Basic three thermodynamic properties functions consists of:

1) Compressibility function:

$$Z(\theta, \pi, r) = \frac{pV}{R_0T} \quad (4.1)$$

2) Enthalpy function:

$$\phi(\theta, \pi, r) = \frac{H}{R_0T} \quad (4.2)$$

3) Entropy function:

$$\psi(\theta, \pi, r) = \frac{S}{R_0} \quad (4.3)$$

where non-dimensional temperature θ , pressure π , air content r are free variables in these functions. More detailed information regard to Zacharias formulas can be found in appendix B. For the further utilization of Zacharias formulas, for instance using in dynamic simulation models of diesel engine performance, the partial derivatives of the properties must be evaluated along with the properties themselves [Valland (1998)]. A subroutine for computation of the properties and their partial derivatives were developed by H. Valland. Afterwards, K. Koosup Yum from Marintek implemented this subroutine into MATLAB. In this master thesis work, MATLAB script of Zacharias formulas is applied to support generating a reference model.

Basically, the subroutine takes $[p, T, F, DCO]$ as input values and computes various properties. The detailed information of input and output parameters are presented in table 4.1 and 4.2:

| Input parameters | Description |
|------------------|---|
| P | Pressure [Pa] |
| T | Temperature [K] |
| F | Fuel-air equivalence ratio [-] ($F = 1/\lambda$) Control parameter: |
| DCO | DCO = 0 ideal gas properties with real gas correction = 1 correction for lower stage dissociation added = 2 correction for upper stage dissociation added |

Table 4.1: Input parameters of the subroutine based on theory of Zacharias formulas

| Output parameters | Description |
|-------------------|--|
| h | specificenthalpy [J/kg] |
| u | specific internal energy [J/kg] specific entropy [J/kgK] |
| s | hp,hT,hF partial derivatives of h with respect to p,T,F. up,uT,uF partial derivatives of u with respect to p,T,F. sp,sT,sF partial derivatives of s with respect to p,T,F. Rp,RT,RF partial derivatives of R with respect to p,T,F. |
| R | gas constant [J/kgK] |
| cp | specific heat at constant pressure [J/kgK] |
| cv | specific heat at constant volume [J/kgK] |
| k | ratio of specific heats: $k=cp/cv$, same as γ |

Table 4.2: Output parameters of the subroutine based on theory of Zacharias formulas

where k in last row of table 4.2 is ratio of specific heats. Among the input parameters, pressure is the measured data from test, temperature can be obtained by estimating model from 2.35. Whereas the fuel-air equivalence ratio is lacked. In next section, obtaining of

equivalence ratio is discovered.

Ordinary differential equations

As Zacharias formulas requires fuel-air equivalence ratio(F) for computing γ , which was not measured in dynamic cycle. To achieve the dynamic F value, integration of ordinary differential equations is carried out. The theory and equations can be found in chapter 2 and equations 2.7 to 2.17.

The ordinary differential equations can be solved by means of numerical integration. MATLAB offers various tools to solve this type of equations. In this work, 'ode45' is chosen as it fits most cases and recommended by developer. It is a solver for solving Non-stiff type problem with a medium order of accuracy. It mainly consists of parts:

- 1) **odefun**: the function handle the right side of differential equations. The equations from matrix 2.17 is implemented.
- 2) **tspan**: a vector specifying the interval of integration.
- 3) **y0**: A vector of initial conditions. In this work, fuel-air equivalence ratio F and temperature T are integrated. The initial value of F for all 7 operating points is set to zero as there is very few fuel in cylinder at the beginning of cycle. The in-cylinder temperature initial value is set to be the temperature at the beginning of integration, which is gained from the mean charge temperature model 2.35 . The detailed initial condition data are shown in table 4.3.

4.2.2 Integrating parameter initialization

To integrate the ordinary differential equations, a set of initial values are carefully chosen.

Integrating range

It is clearly that mean charge temperature has less significant impact on γ value in lower value. Therefore, the focus does not lie on the inlet and exhaust stroke in this work. Besides, the ode function was designed for the valve-closed part of cycle. The pressure and ROHR data are required as reference data by ode function. The range of integration should not exceed the range of reference data. Based on all above, it is decided that the integrating range lies on the a bit behind inlet valve closing time and before the exhaust valve opening time, which is [280, 520] CAD.

Reference Data Range

As mentioned, the dynamic pressure and ROHR are required by ode function for the use of integration. The range of reference data should be wider than integration range. Therefore, the region of [275, 525] CAD is adopted as a safe range because valve timing of Scania engine remains unknown.

Integrating initial condition

A vector of parameter value at the beginning of integration are required, consists of temperature, fuel-air equivalence ratio, pressure, cylinder volume, mass of trapped air. The determination of these parameters can be gained from measuring, estimating and computing. All the initial condition and parameters are list in table 4.3.

| Items | Units | Value | Source |
|-------------------|-----------|------------|----------------------|
| P0 | [Pa] | 601087 | Measuring data |
| T0 | [K] | 437.3 | Estimating model2.35 |
| F0 | [-] | 0 | - |
| V0 | [m^3] | 0.001 | equation2.24 |
| M_a | kg | 0.0049 | equation2.3 |
| Integration Range | [CAD] | [280, 520] | - |
| Reference Range | [CAD] | [275, 525] | - |

Table 4.3: Initial condition data for integration of ordinary differential equations

4.2.3 Iterating process

After integrating the differential equations, an initial set of γ are gained. To ensure a steady and accurate reference model, an iteration process is carried out and demonstrated in figure 4.6. Firstly, the rate of heat release is calculated by constant-value γ model and it is used in solving ordinary differential equations. After differential equations are integrated by ode solver, a set of temperature and fuel-air equivalence ratio vectors are gained. Later, these temperature and equivalence ratio vectors together with measured pressure data are inserted into Zacharias formulas and yield first set of reference γ model. For minimizing the error, an iterating process is adopted: the obtained γ model is inserted back into computation of ROHR, which yields a new set of ROHR value. The new set of ROHR is used to replace origin when solving ordinary differential equations. The iteration process stops when the reference model data is converged.

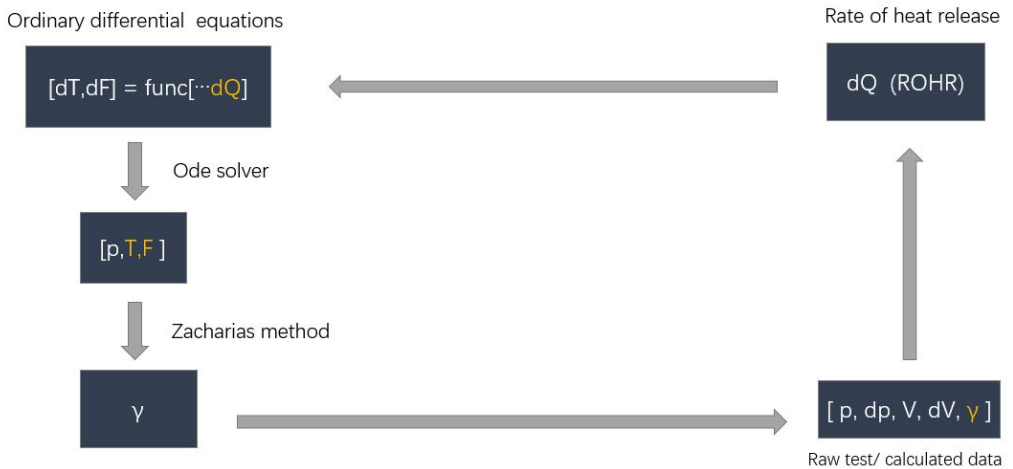


Figure 4.6: Reference model iterating process loop

Converge criteria

To ensure the convergence of reference model, MRE (Maximum relative error) is used to measure the difference during the iterating. The relative error is the absolute error divided by actual measurement (in here refers to reference model). When the MRE of reference model is no higher than 0.1%, the model is considered at convergence.

4.2.4 Results demonstration

After 3-time iterating, the γ model reached the convergence. In this section, a set of results at full-load test point (220kW/1800RPM) are demonstrated as an example.

Temperature model retrofit

In Chapter 2, an in-cylinder temperature estimating model proposed by [Gatowski et al. (1984)] is introduced and used to compute γ models value. However, this estimating model is built based on the assumption of gas constant R remaining constant during the cycle. As a matter of fact, R value varies within one cycle, which means the in-cylinder temperature model 2.35 is not accurate.

On the other hand, during the computation of the reference model, the R value is obtained from Zacharias formulas, in which considering the impact of factors (temperature, pressure and fuel-air equivalence ratio). Therefore, after reference model reached the convergence, the comparison between initial temperature model and retrofit temperature model are shown in figure 4.7. As can be observed, at full load test point, the value of reference temperature model is significant higher than that of initial estimating model.

Dynamic fuel-air equivalence ratio

There is no available direct method measuring the dynamic F value within current condition. To supply F value as input value for Zacharias formulas, dynamic fuel-air equivalence ratio is computed by integrating the ordinary differential equations. The results

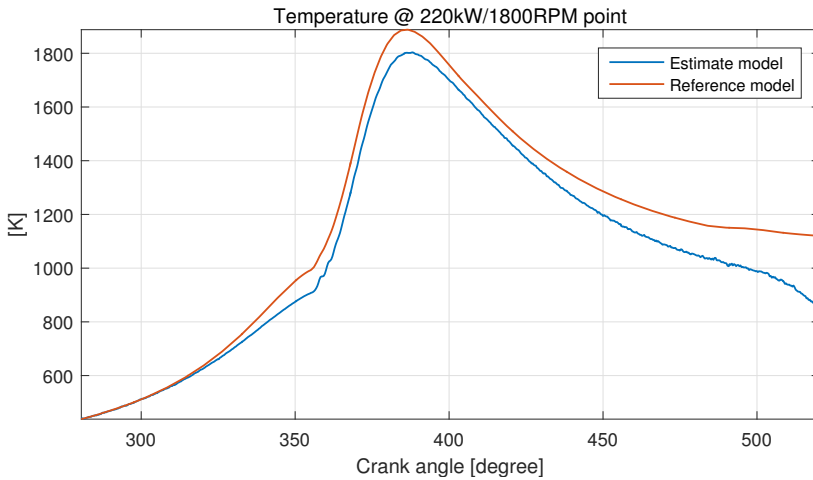


Figure 4.7: Comparison of estimate temperature model and reference model @220kW/1800RPM condition

after reaching the convergence is shown in figure 4.8. The fuel-air equivalence ratio starts to increase from zero with the beginning of fuel injection and ends up with stabilizing at approximately 0.46, indicating a typical lean combustion of diesel engine.

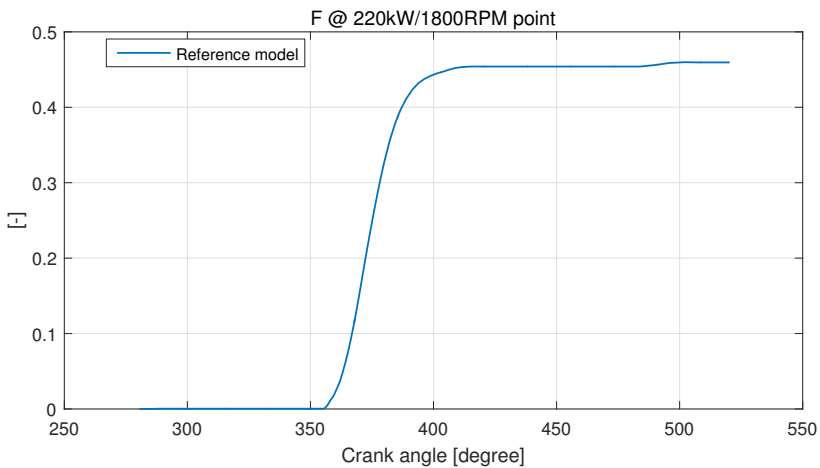


Figure 4.8: Dynamic fuel-air equivalence ratio model gained from reference model @220kW/1800RPM condition

Reference γ Model

After 3-time iteration, the reference γ model finally achieves a MRE value at 0.1%, which considered as converged state. Figure 4.9 shows the how γ model varies during the iteration. It is found that after first iteration the most significant difference on reference model occurs. The reference model shows a strong tendency of convergence after second and third iteration, as can be observed as yellow and purple line on the figure 4.9.

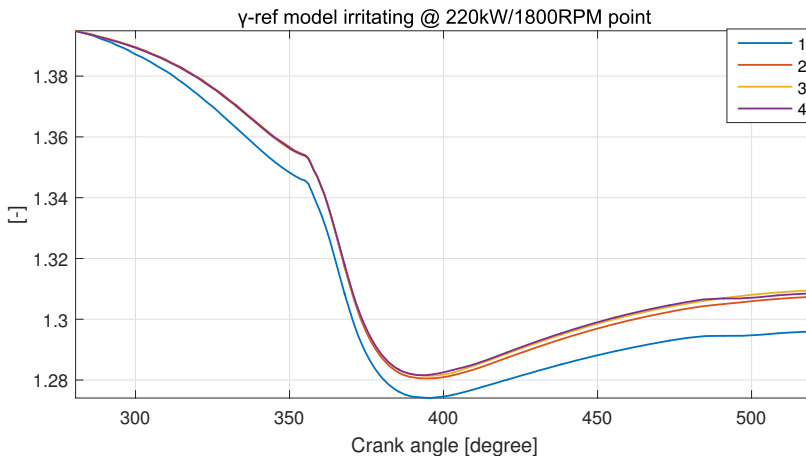


Figure 4.9: Comparison of reference γ models during the iterating process @220kW/1800RPM condition, the purple line is considered as at converged state.

Impact on ROHR

After the converged reference γ model is obtained, ROHR applying reference γ model is plot against the ROHR computed by constant value γ model. From figure 4.10, it is easily found that constant-value γ model leads to an apparent higher ROHR value at end of compression stroke and power stroke. Especially in terms of peak value, it caused a maximum difference of ROHR, with roughly 25[J/degree].

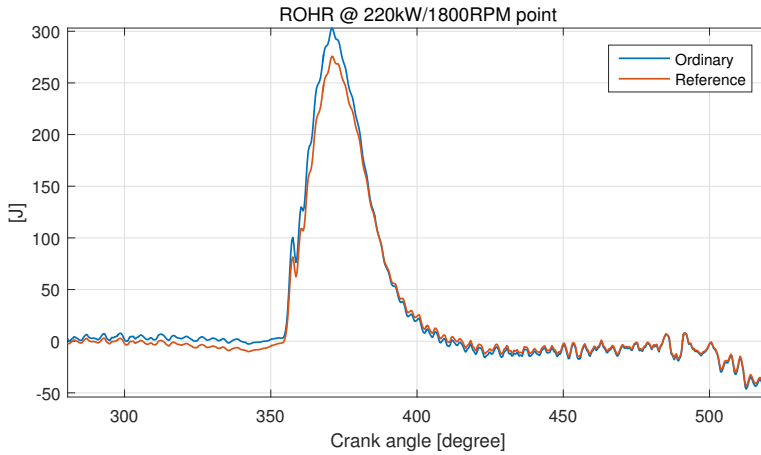


Figure 4.10: Comparison of ROHR computed by original constant-value γ model and reference γ model @220kW/1800RPM condition

4.3 Model Evaluation

With the reference model obtained, the existing temperature-dependent γ models are evaluated in this section. The evaluation also comprises the γ 's impact on ROHR and the range of evaluation covers all test points within E2 and E3 cycles. Two test cycles are weighed equally in evaluation for giving a comprehensive indication at all conditions. The results of overall 7 test points are presented and discussed. Certain statistical criteria are applied on γ domain and ROHR domain.

4.3.1 Evaluation criteria

γ model

Three γ models are evaluated by comparing with reference model in terms of 2 criteria:

- Maximum relative error (MRE), which yields the maximum error between γ model candidates and reference model.
- Normalized root mean square error (NRMSE), this criteria measures the mean error between γ model candidates and reference model.

| Test point | kW/RPM | MRE [%] | MRE[%] | MRE[%] |
|------------|----------|-----------------|--------------|---------------|
| | | Gatowskis model | Brunts model | Egnells model |
| 1 | 220/1800 | 3.75 | 6.17 | 4.18 |
| 2 | 165/1800 | 3.80 | 6.25 | 4.26 |
| 3 | 110/1800 | 3.79 | 6.26 | 4.07 |
| 4 | 55/1800 | 3.74 | 6.24 | 3.88 |
| 5 | 165/1638 | 3.72 | 6.15 | 4.07 |
| 6 | 110/1440 | 3.59 | 5.99 | 3.76 |
| 7 | 55/1134 | 3.46 | 5.81 | 3.51 |
| Mean value | | 3.69 | 6.12 | 3.96 |

Table 4.4: Maximum relative error(MRE) of three γ model candidates at all test points

ROHR domain

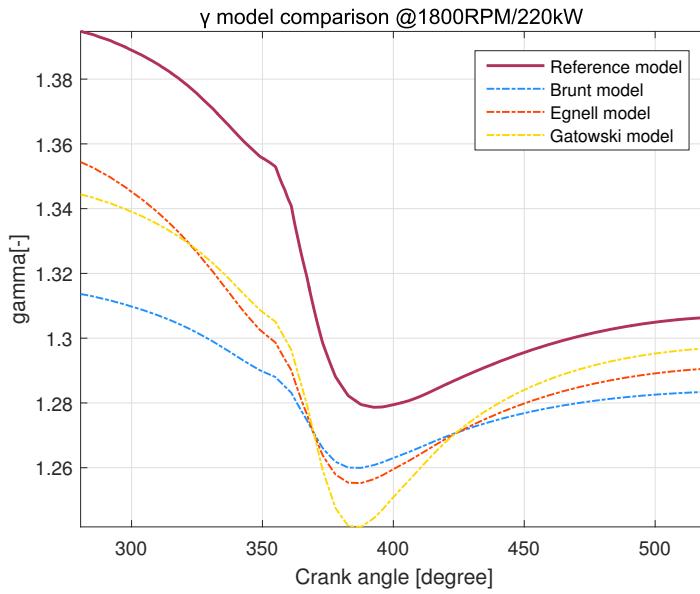
Root mean square error (RMSE) normally demonstrates the mean absolute error. It is used here to measure the error of ROHR caused by γ model. This will be helpful to indicate the superiority of γ model.

4.3.2 Results analysis

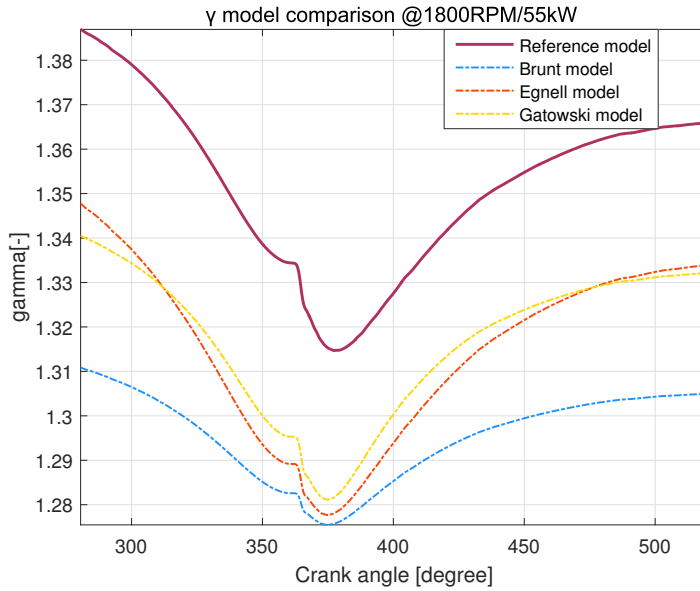
γ -domain

The reference γ model at all 7 test points are plotted against three other γ models. Figure 4.11 is demonstrated as examples here, other comparisons can be found in appendix A. As can be seen from figure, the reference model value is significant higher than candidates yet sharing a very similar trace with the other three model candidates during whole cycle. This phenomenon could be attributed to the fact that the fuel-air equivalence ratio in Scania engine is much lower than that three model candidates were designed for.

The evaluation results in terms of MRE and NRMSE are present in table 4.4 and 4.5. As can be observed easily, in terms of maximum relative error, the Gatowski's model yields the best fitting effect at all the test points. The Egnell's model has a very closing results to Gatowski's model, while Brunt's model achieve the most unsatisfied output, with almost twice maximum relative error of Gatowski's model.



(a) @100%speed/100%load operating condition



(b) @100%speed/25%load operating condition

Figure 4.11: Two examples of evaluation of three γ model candidates by comparing with reference model.

| Test point | kW/RPM | NRMSE [%] Gatowskis model | NRMSE [%] Brunts model | NRMSE [%] Egnells model |
|------------|----------|------------------------------|---------------------------|----------------------------|
| 1 | 220/1800 | 1.53 | 1.40 | 1.37 |
| 2 | 165/1800 | 1.57 | 2.18 | 1.83 |
| 3 | 110/1800 | 2.27 | 3.36 | 2.68 |
| 4 | 55/1800 | 3.42 | 5.32 | 3.95 |
| 5 | 165/1638 | 1.68 | 1.99 | 1.81 |
| 6 | 110/1440 | 2.56 | 3.34 | 2.93 |
| 7 | 55/1134 | 3.71 | 5.17 | 4.34 |
| Mean value | | 2.39 | 3.25 | 2.70 |

Table 4.5: Normalized root mean square error (NRMSE) of three γ model candidates compared with reference model at all test points

Unlike MRE indicates the maximum error, NRMSE evaluates the mean error during the cycle. It is obviously found that Gatowski's model having closest results with reference data at 5 points and Egnell's model perform best in the rest of two points. Still, the output yield by Gatowski's model and Egnell's model are highly close, not exceeding 0.1. On the other hand, Brunt's model has a much worse fitting.

ROHR domain

The purpose of improving quality of γ model is to enhance the accuracy of the RHOR. Therefore, it is necessary to evaluate the difference of the ROHR computed by different γ models.

The comparison of ROHR computed with different γ models is plotted in figure 4.12. As observed, it can be found that the ROHR applying reference γ model owns a higher peak value than that of other ROHR curves. The necessary quantified evaluation in terms of RMSE is shown in the table 4.6. According to the data from table, Gatowski's model yields the least RMSE value at most of test points except for full-load point where Egnell's model gives the best performance. Similarly, Brunt's model does not perform good in computing ROHR as it gives out obvious higher RMSE than other two γ models.

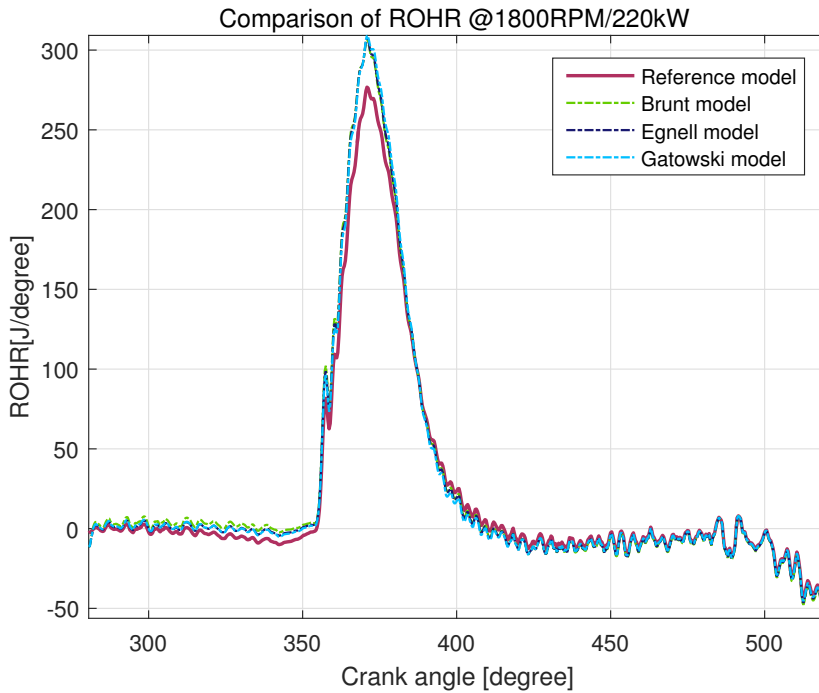


Figure 4.12: Comparison of ROHR applying γ model candidates and reference model @220kW/1800RPM

From comparison in ROHR domain, it is concluded that the difference caused by γ models mainly located in the combustion region. Inspired by this finding and the fact of similarity between the reference γ model and candidate models, a retrofit γ model is proposed in the next section.

4.4 A Retrofit γ Model

It is found that the reference γ Model has a very similar trace with candidates, while the difference in absolute value is existing. To further improve the accuracy of γ model and obtain a more accurate model for Scania engine, a set of offset are proposed in this section. The γ model candidate applies with offset values is called retrofit model.

| Test point | kW/RPM | Gatowski RMSE [J/deg] | Brunt RMSE [J/deg] | Egnell RMSE [J/deg] |
|------------|----------|--------------------------|-----------------------|------------------------|
| 1 | 220/1800 | 8.48 | 8.70 | 8.17 |
| 2 | 165/1800 | 5.30 | 7.83 | 6.24 |
| 3 | 110/1800 | 5.08 | 7.57 | 5.92 |
| 4 | 55/1800 | 4.65 | 6.93 | 5.27 |
| 5 | 165/1638 | 6.24 | 7.79 | 6.84 |
| 6 | 110/1440 | 4.80 | 6.38 | 5.44 |
| 7 | 55/1134 | 3.85 | 5.26 | 4.37 |
| Mean value | | 5.48 | 7.21 | 6.04 |

Table 4.6: Root mean square error (RMSE) of ROHR computed by three γ model candidates compared with one computed by reference model

Evaluation range

The purpose of improving accuracy of γ model is to improve the accuracy of ROHR. Based on the evaluation of impact on ROHR given by different γ models, the significant difference on ROHR mainly lies on combustion process, which is considered as the most important part in the heat release analysis. Therefore, the variance in the range outside combustion process is neglected and the evaluation range is redetermined as [350, 420] CAD.

γ offset

As observed from figure 4.11, reference model owns a similar trace with model candidates while there is a significant absolute error existing. To further improve the model accuracy, a set of γ offset are proposed in this work. The γ offset is determined by mean error between candidate models and reference model during one cycle. Table 4.7 demonstrates the results of all test points. As the purpose is trying to achieve equal improvement for all operating conditions, it is decided that the mean error among 7 test points is used as offset value for each model. As observed, Gatowski's model gives out the minimum mean error of 0.03 while Brunt's model and Egnell's model give clearly higher error of 0.039 and 0.033, respectively.

| Test point | kW/RPM | Mean error Gatowski's model | Mean error Brunt's model | Mean error Egnell's model |
|------------|----------|--------------------------------|-----------------------------|------------------------------|
| 1 | 220/1800 | -0.0325 | -0.0247 | -0.0267 |
| 2 | 165/1800 | -0.0284 | -0.0400 | -0.0338 |
| 3 | 110/1800 | -0.0292 | -0.0443 | -0.0353 |
| 4 | 55/1800 | -0.0330 | -0.0519 | -0.0383 |
| 5 | 165/1638 | -0.0278 | -0.0315 | -0.0297 |
| 6 | 110/1440 | -0.0284 | -0.0371 | -0.0328 |
| 7 | 55/1134 | -0.0307 | -0.0433 | -0.0361 |
| Mean value | | -0.0300 | -0.0390 | -0.0333 |

Table 4.7: Mean error of three γ model candidates comparing to reference model

As the offset value is determined by the mean error of 7 test points, the retrofit models may not fit well with reference model in every operating condition. It is clearly found from figure 4.13 that retrofit models fit much better in 1134RPM/55kW than in full-load condition. The evaluation of retrofit model is present later.

4.4.1 Results evaluation

γ -domain

Comparison in terms of Maximum relative error(MRE) of three retrofit candidate models is demonstrated in table 4.8, retrofit Gatowski's model yields least MRE in all 7 operating condition, mean value at 1.103%. Egnell's model and Brunt's model reach apparent higher mean MRE value at 1.35% and 1.78%, respectively. Table 4.9 summarizes the evaluation of three retrofit models by means of NRMSE. It is clearly seen that Gatowski's model having the best fitting performance at 5 of overall 7 test points, only at test point 36 (110kW/1134RPM) Egnell's model achieves the best goodness of fitting. The mean value of retrofit model's MRE & NRMSE at 7 test points are compared with that of original candidate models in the range of [355,420] CAD. The results are shown in the bar graph 4.14, from which it can be concluded that three candidate models achieve the significant improvements on fitting with reference model after applying the γ -offset. Obviously, Gatowski's model gives the least value at both two criteria, thus retrofit Gatowski's model

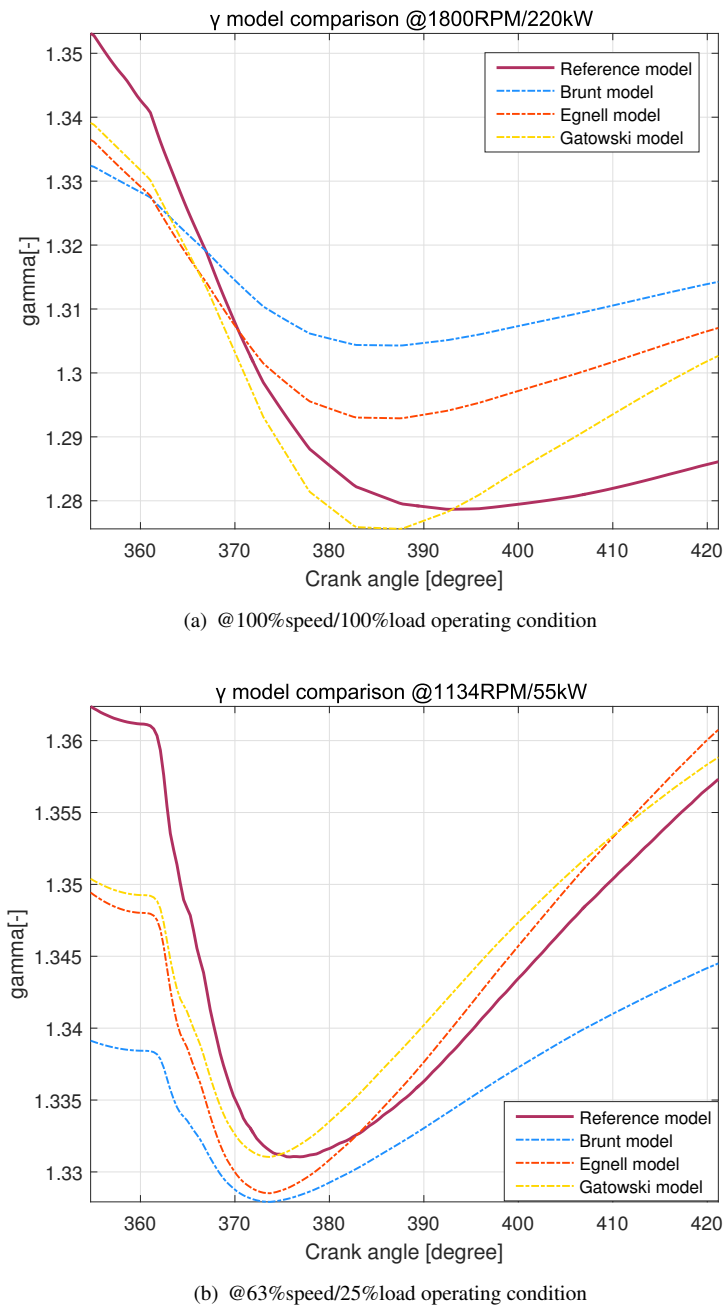


Figure 4.13: Two examples of comparison of three retrofit γ models with reference model

is chosen as the final γ model which will implement in ROHR computation module of Scania engine.

| Test point | kW/RPM | MRE[%] | MRE[%] | MRE[%] |
|------------|----------|------------------|---------------|---------------|
| | | Gatowski's model | Brunt's model | Egnel's model |
| 1 | 220/1800 | 1.114 | 1.781 | 1.350 |
| 2 | 165/1800 | 1.422 | 2.097 | 1.654 |
| 3 | 110/1800 | 1.302 | 2.131 | 1.488 |
| 4 | 55/1800 | 1.172 | 2.107 | 1.305 |
| 5 | 165/1638 | 1.117 | 1.631 | 1.362 |
| 6 | 110/1440 | 0.911 | 1.375 | 1.155 |
| 7 | 55/1134 | 0.687 | 0.973 | 0.906 |
| Mean value | | 1.103 | 1.781 | 1.350 |

Table 4.8: Mean value of MRE among all test points between original γ model candidates and retrofit model candidates

| Test point | kW/RPM | NRMSE | NRMSE | NRMSE |
|------------|----------|------------------|---------------|---------------|
| | | Gatowski's model | Brunt's model | Egnel's model |
| 1 | 220/1800 | 0.39 | 1.00 | 0.65 |
| 2 | 165/1800 | 0.65 | 0.80 | 0.65 |
| 3 | 110/1800 | 0.70 | 0.79 | 0.66 |
| 4 | 55/1800 | 0.53 | 1.08 | 0.57 |
| 5 | 165/1638 | 0.58 | 0.91 | 0.66 |
| 6 | 110/1440 | 0.72 | 0.86 | 0.69 |
| 7 | 55/1134 | 0.59 | 0.52 | 0.60 |
| Mean value | | 0.59 | 0.85 | 0.63 |

Table 4.9: Normalized root mean square error(NRMSE) between original γ model candidates and retrofit model candidates

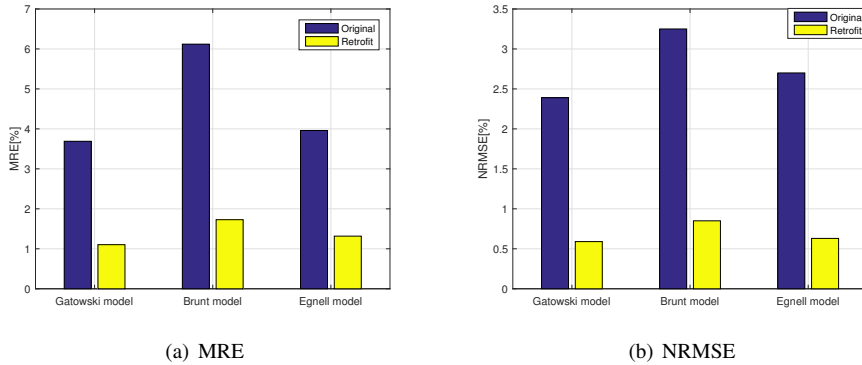


Figure 4.14: Comparison of MRE & NRMSE among all test points between original γ model candidates and retrofit model candidates

ROHR domain

As known, the Scania engine used to compute ROHR by applying constant-value γ model. To evaluate the improvement in ROHR computation by applying new retrofit gatowski's model, the RMSE criteria is carried out and results is shown in table 4.10. Assuming the reference model is accurate, ROHR computed with applying retrofit gatowski's model shows a relatively stable error(RMSE) among 7 test points with a mean value of 1.704 [J/deg]. On the other side, ROHR compute with the constant-value γ model has a intuitive higher mean RMSE value at 14.476 [J/deg]. In general, the RMSE of ROHR applying retrofit Gatowski's model has been reduced by over 80% at all test points. The reduced part is decreasing with lower load conditions especially in E2 cycle. This phenomenon could be explained by higher in-cylinder temperature caused by higher load and the effect of temperature-dependent part in Gatowski's model is growing, which may lead a lower γ value and higher error in ROHR computation. Overall, in the range of all 7 operating conditions, the retrofit Gatowski's model eliminate 88% of RMSE comparing to original γ model.

The ROHR comparison at full-load point is plotted as an example in figure 4.15, it is clearly to find that ROHR curve computed with original model starts to have lower ROHR

| Test point | kW/RPM | RMSE of ROHR constant-value γ [J/deg] | RMSE of ROHR Gatowski's model [J/deg] | Improvement [%] |
|------------|----------|--|---|--------------------|
| 1 | 220/1800 | 2.803 | 24.694 | 88.647 |
| 2 | 165/1800 | 1.752 | 14.594 | 87.994 |
| 3 | 110/1800 | 1.522 | 11.622 | 86.904 |
| 4 | 55/1800 | 1.363 | 8.174 | 83.323 |
| 5 | 165/1638 | 1.984 | 18.868 | 89.484 |
| 6 | 110/1440 | 1.405 | 13.807 | 89.824 |
| 7 | 55/1134 | 1.099 | 9.576 | 88.519 |
| Mean value | | 1.704 | 14.476 | 88.228 |

Table 4.10: comparison of Root mean square error(RMSE) of ROHR between one computed by constant-value γ model and computed by retrofitted Gatowski's model

value from TDC, especially with around 50 [J/deg] error at peak value. While after passing 390 CAD, it shows a roughly 15 [J/deg] higher value than reference model. This error can cause nonnegligible effect during the heat-release analysis. Whereas the ROHR computed with retrofit Gatowski's model has a much more similar trace with reference model during the whole range.

The retrofit Gatowski's model is rewrite as:

$$\gamma_{lin}(T) = 1.405 - 6.99 * 10^{-5} * T \quad (4.4)$$

For the simplicity of computation and being able to apply in real-time computation module, model 2.35 is used to estimate in-cylinder temperature. The differential between reference temperature model and estimating model 2.35 shown in figure 4.7 leads to negligible error because the magnitude of differential largely reduced when it reflects on γ model.

$$T = \frac{T_{ref}}{p_{ref} V_{ref}} pV$$

where the reference position is set at 180 CAD, a vector of reference data supplied by Laboratory. T_{ref} is set as 315K, V_{ref} is given as $0.002m^3$ and p_{ref} can measured by pressure sensor.

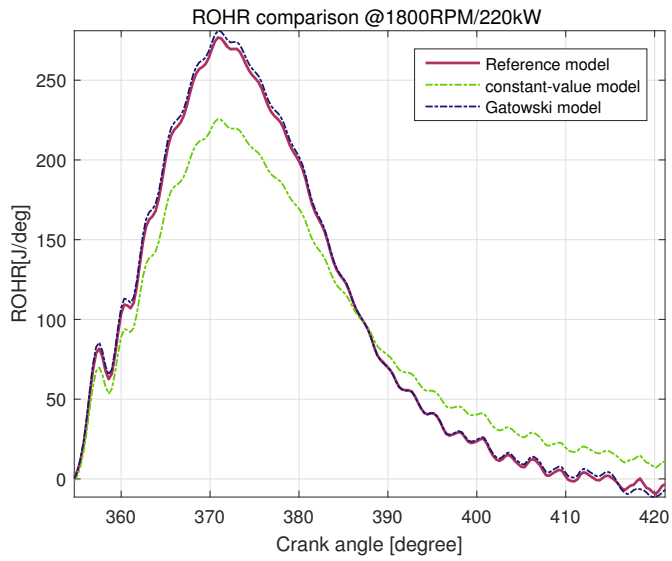


Figure 4.15: Comparison between ROHR computing by constant-value γ model and retrofitted Gatowski' model @220kW/1800RPM condition

Conclusion

5.1 Model candidates evaluation

To improve the accuracy of ROHR computation, three existing temperature-dependent γ models are evaluate in this work. Based on theory of ordinary differential equations and Zacharias's thermodynamic formulas, a reference γ model is built up for evaluating the candidates. The evaluation is carried out in two domains: ratio of specific heats and ROHR calculated with corresponding γ models.

In γ -domain, the Gatowski's model achieves the closest results with reference model in both maximum relative error(MRE) and normalized root mean square error(NRMSE) among most of test points. The Egnell's model performs nearly same good as Gatowski's model while Brunt's model has a significant higher error in both two criteria. In ROHR domain, the ROHR applying Gatowski's model gains the least RMSE level at 5.48[J/deg], the Brunt's model and Egnell's model give 31.5% and 10.1% higher RMSE, respectively.

5.2 Retrofit model

It is observed that the candidate γ models having a high level of similarity with reference model in trace shape while the absolute-value error is existed. To maximally eliminate the effect of this absolute error, a set of γ value offsets are applied in the candidate models. The same evaluation criteria (MRE, NRMSE and RMSE) are adopted for evaluating retrofit models and the evaluation range is shrunk to [355, 420] CAD in order to emphasize in the region of combustion process, where gives the most significant difference on ROHR computation. The mean error between model candidates and reference model among all 7 test points are used as the offset values. The model candidates with applying γ -offset are called retrofit models. The evaluation of retrofit model candidates are adopted in same two domains. In γ domain, the retrofit Gatowski's model yields the best results in both RME and NMRSE criteria. Therefore, it is decided that the retrofit Gatowski's model being chosen applying for future ROHR computation in NTNU machinery laboratory. By comparing the ROHR results calculated by retrofit gatowski's model and original constant-value γ model, root mean square error (RMSE) is significantly reduced by average 88% in all 7 test points.

5.3 Future work

The retrofitting method is relatively simple by just applying an offset value due to time limitation, more work should be put into building a new empirical model by using some certain tools. Besides, The candidate models chose here are all temperature-dependent for the simplicity of calculation, so it can be applied in real-time computation system. While actually other factors like air-fuel ratio, pressure, etc. also have impact on ratio of specific heats. Some higher order polynomial γ model which considers the effect of those factors can be also worked out and compared. More efforts could emphasize in the influence of those factors individually.

Bibliography

Brunt, M. F., Rai, H., Emtage, A. L., 1998. The calculation of heat release energy from engine cylinder pressure data. Tech. rep., SAE Technical Paper.

Bueno, A. V., Velásquez, J. A., Milanez, L. F., 2012. Internal combustion engine indicating measurements. Edited by Md. Zahurul Haq, 23.

Chun, K. M., Heywood, J. B., 1987. Estimating heat-release and mass-of-mixture burned from spark-ignition engine pressure data. *Combustion Science and Technology* 54 (1-6), 133–143.

Egnell, R., 1998. Combustion diagnostics by means of multizone heat release analysis and no calculation. Tech. rep., SAE Technical Paper.

Engineering, L., 2013. First Law of Thermodynamics for an Open System. <http://www.learnengineering.org/2013/03>, [Online; accessed 19-March-2013].

Gatowski, J., Balles, E. N., Chun, K., Nelson, F., Ekchian, J., Heywood, J. B., 1984. Heat release analysis of engine pressure data. Tech. rep., SAE Technical paper.

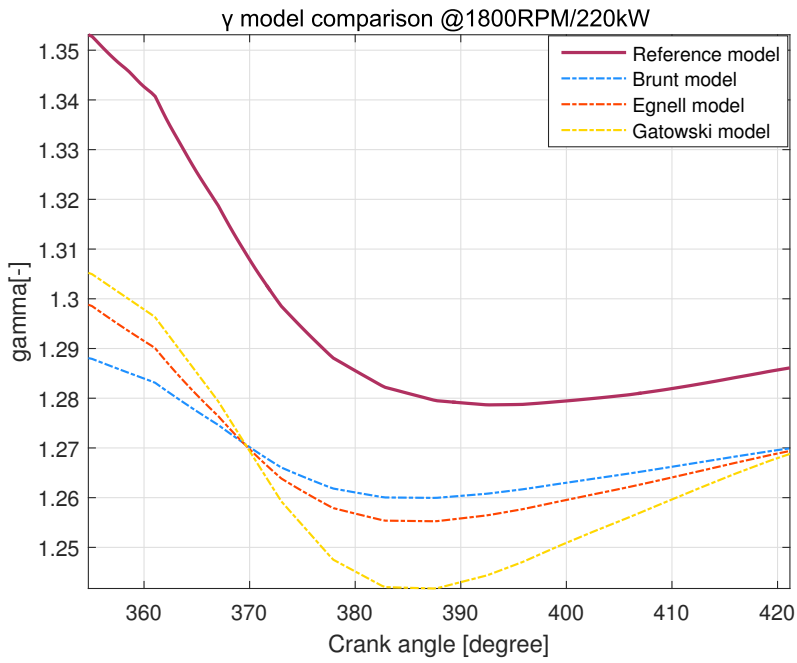
Hatlevold, E. S., 2010. Assessment of engine performance and exhaust emission at changing operating conditions and under fault conditions.

Heywood, J., 1988. *Internal combustion engine fundamentals*. McGraw-Hill Education.

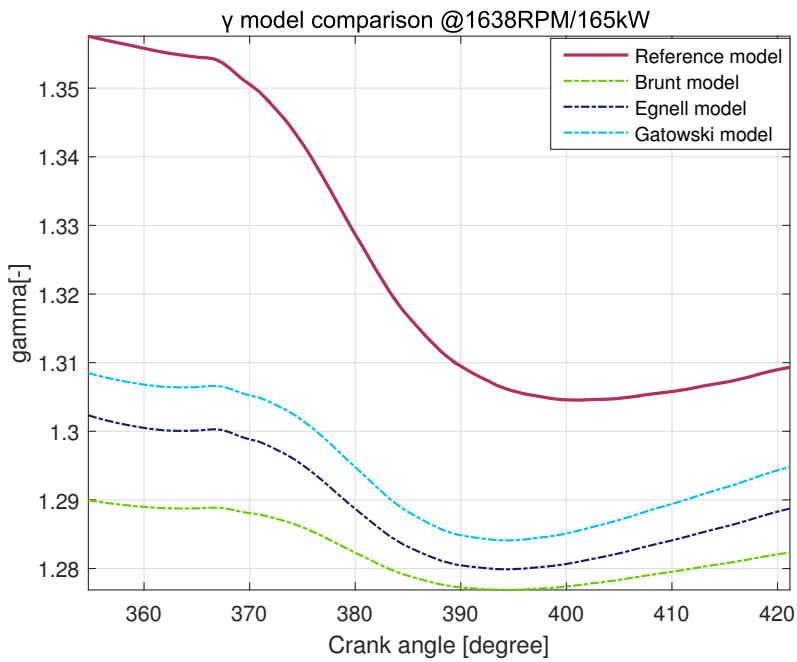
-
- Klein, M., 2004. A specific heat ratio model and compression ratio estimation. Division of Vehicular Systems, Department of Electrical Engineering, Linköping University.
- Marzouk, M., Watson, N., 1976. Some problems in diesel engine research with special reference to computer control and data acquisition. Proceedings of the Institution of Mechanical Engineers 190 (1), 137–151.
- Valland, H., 1998. Thermodynamic properties of combustion gases according to zacharias. Tech. rep., Department of Marine Engineering NTNU.
- Zhen, D., Wang, T., Gu, F., Tesfa, B., Ball, A., 2013. Acoustic measurements for the combustion diagnosis of diesel engines fuelled with biodiesels. Measurement Science and Technology 24 (5), 055005.

Plot of results

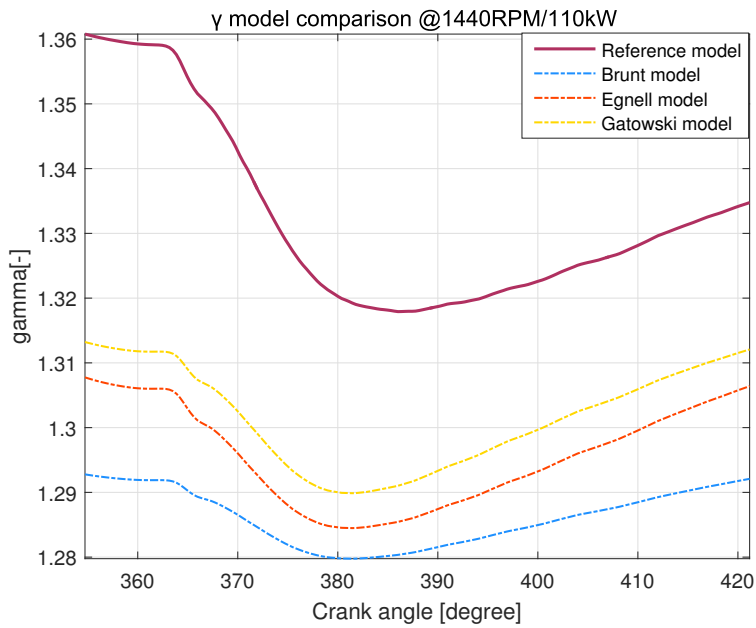
In this chapter, the original γ model candidates and retrofit γ model candidates are both compared with reference model and present in this chapter. To demonstrate the impact on ROHR computation, ROHR calculated by original constant-value γ model and retrofit Gatowski's model are compared and present.



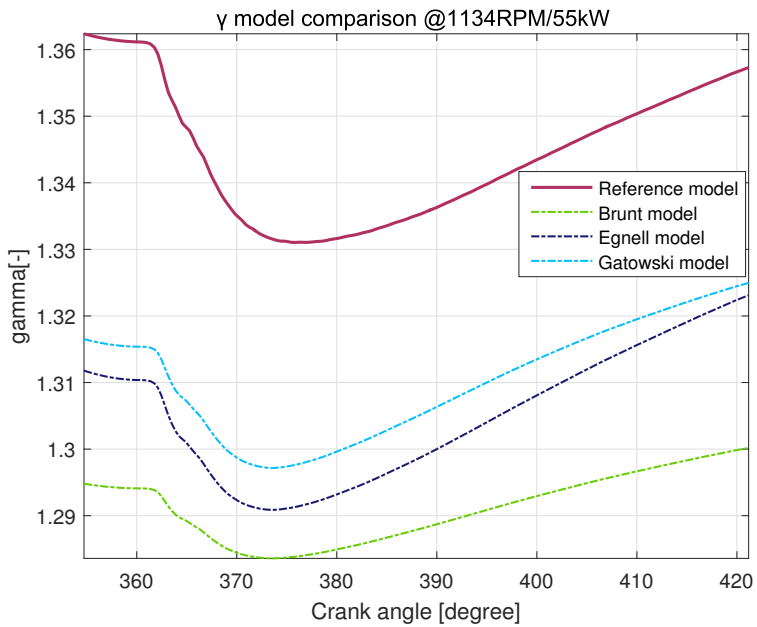
(a) 100%load / 100%speed



(b) 75%load/ 100%speed

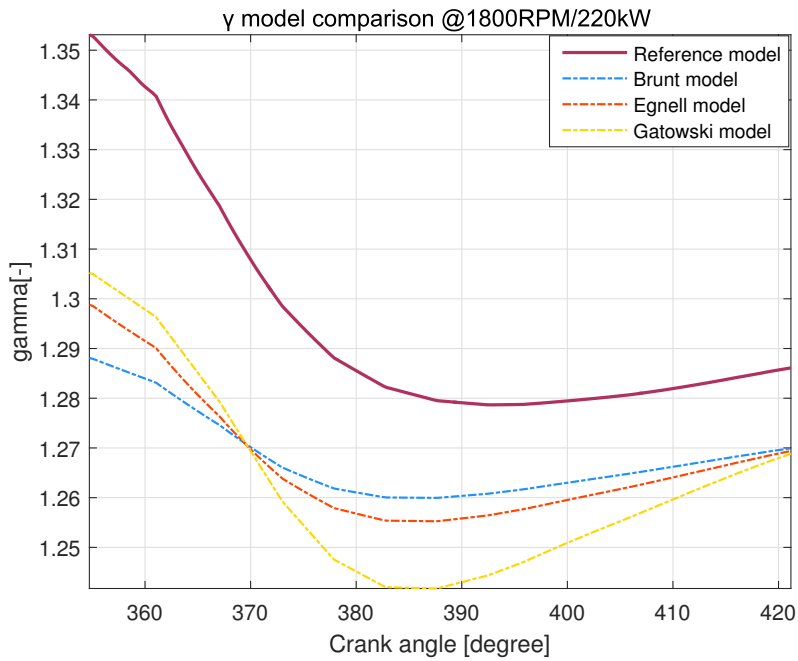


(c) 50%load/ 100%speed

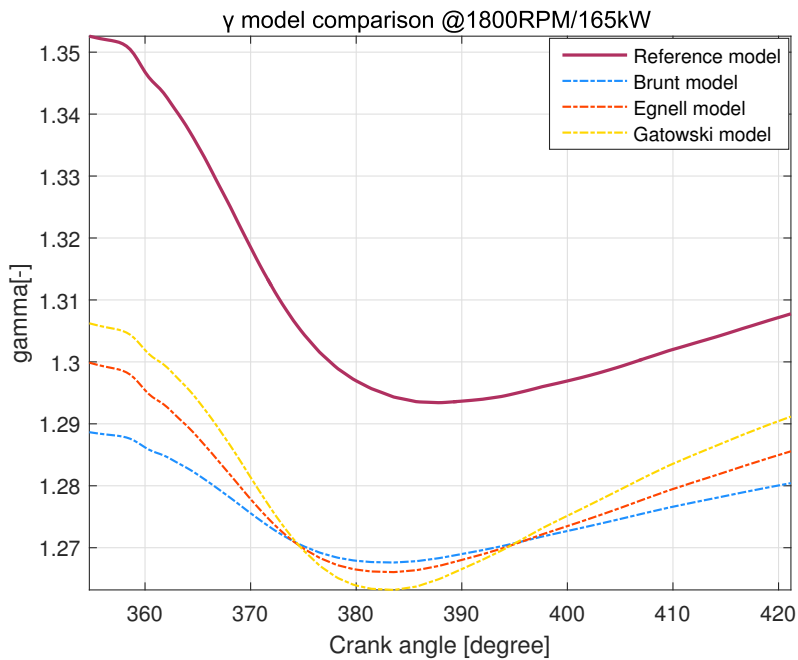


(d) 25%load/ 100%speed

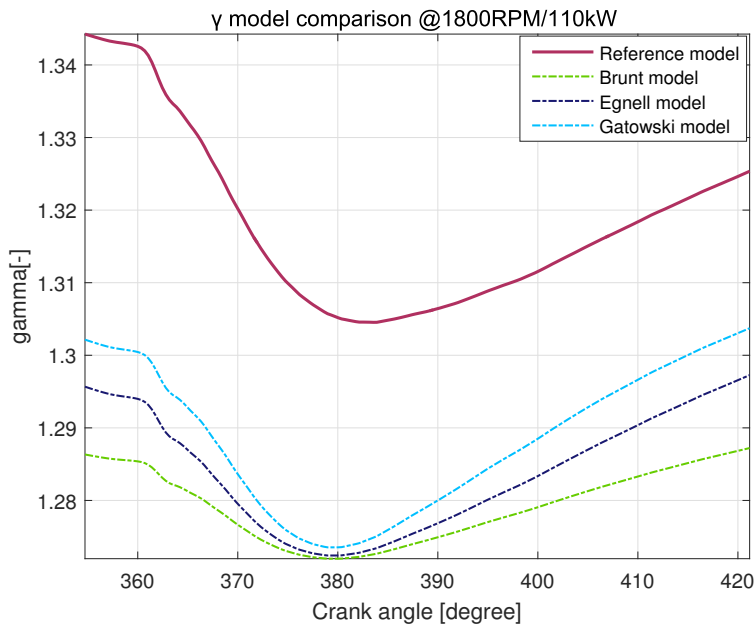
Figure A.1: Original γ model candidates comparison in *E2* cycle



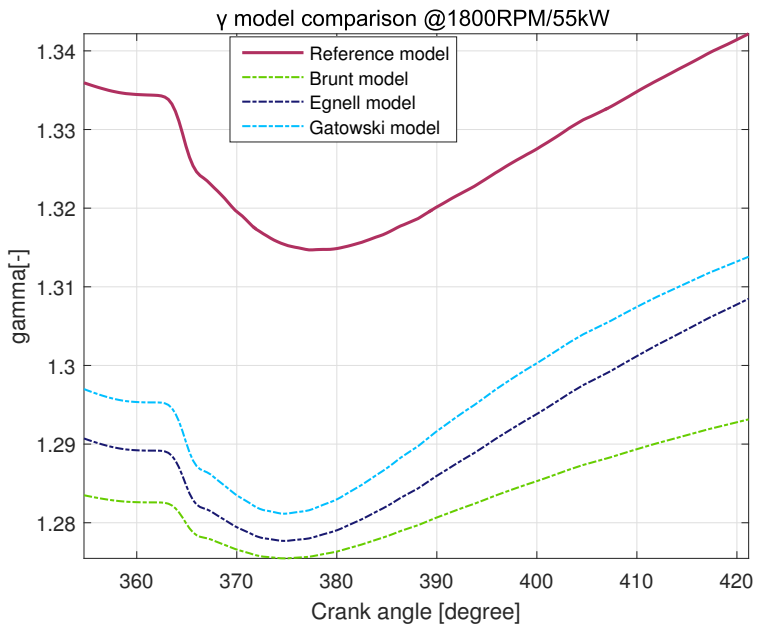
(a) 100%load / 100%speed



(b) 75%load/ 91%speed

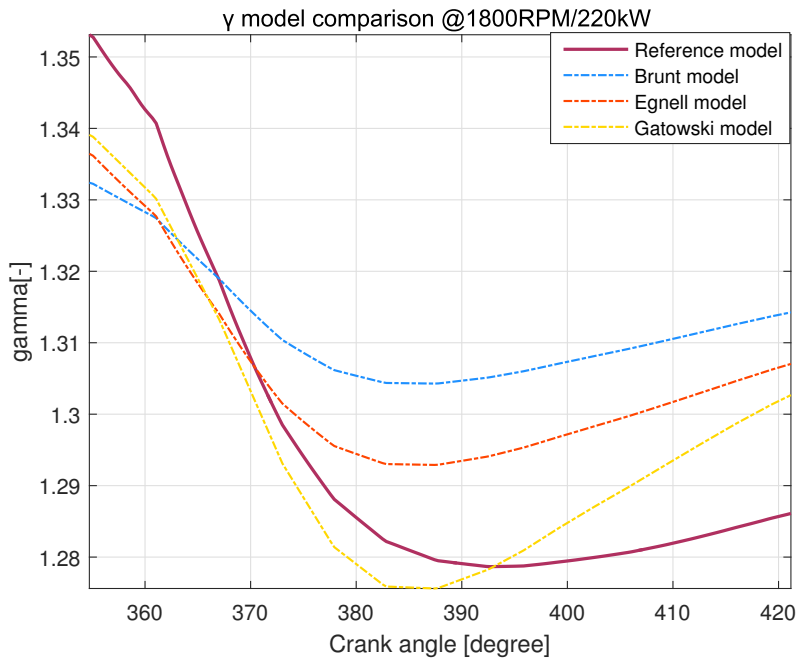


(c) 50%load/ 80%speed

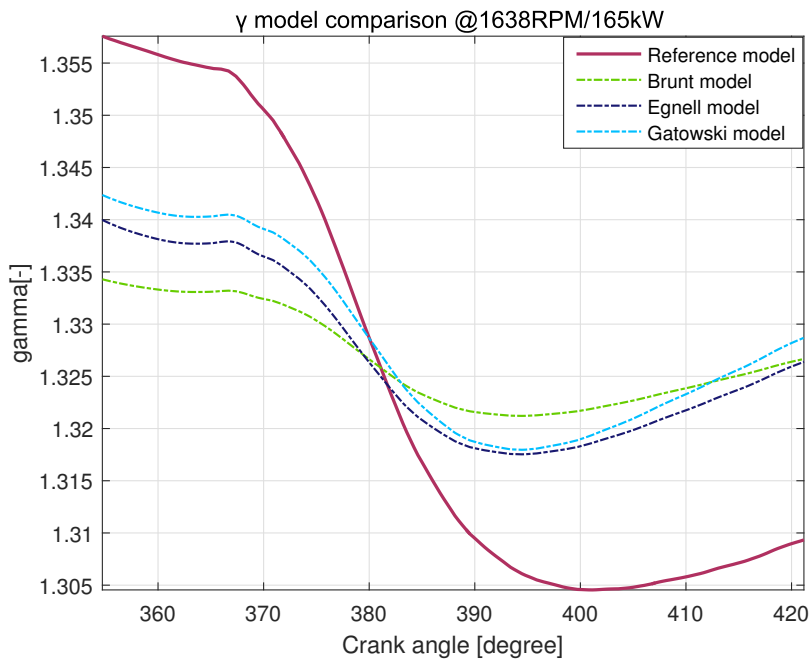


(d) 25%load/ 63%speed

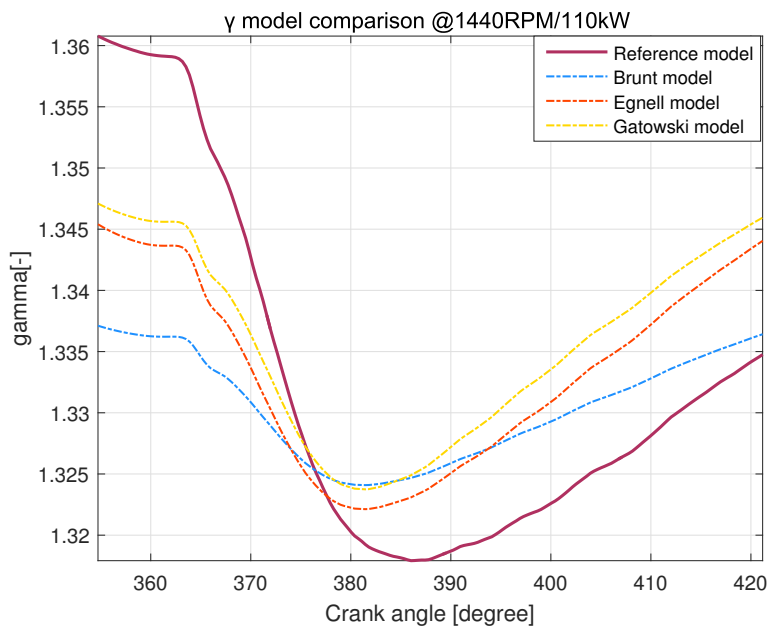
Figure A.2: Original γ model candidates comparison in *E3* cycle



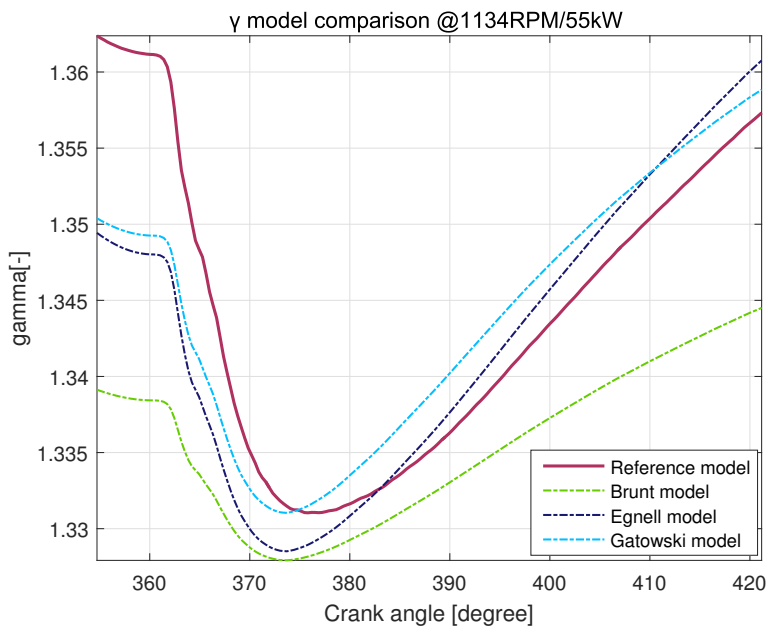
(a) 100%load / 100%speed



(b) 75%load/ 100%speed

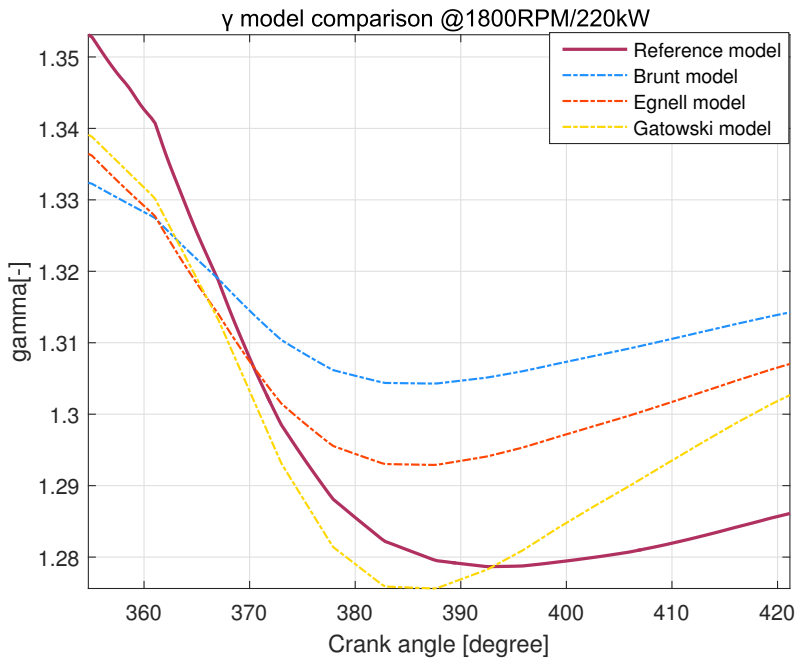


(c) 50%load/ 100%speed

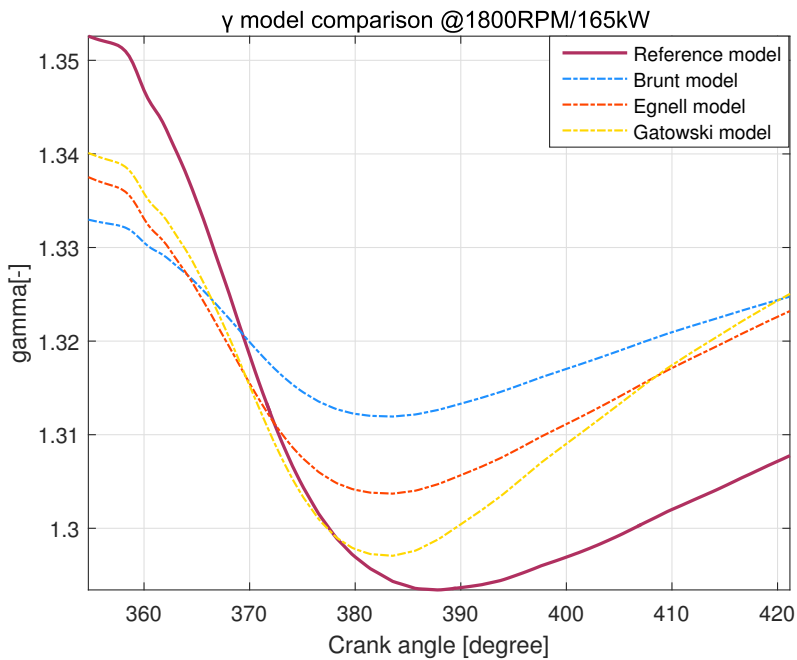


(d) 25%load/ 100%speed

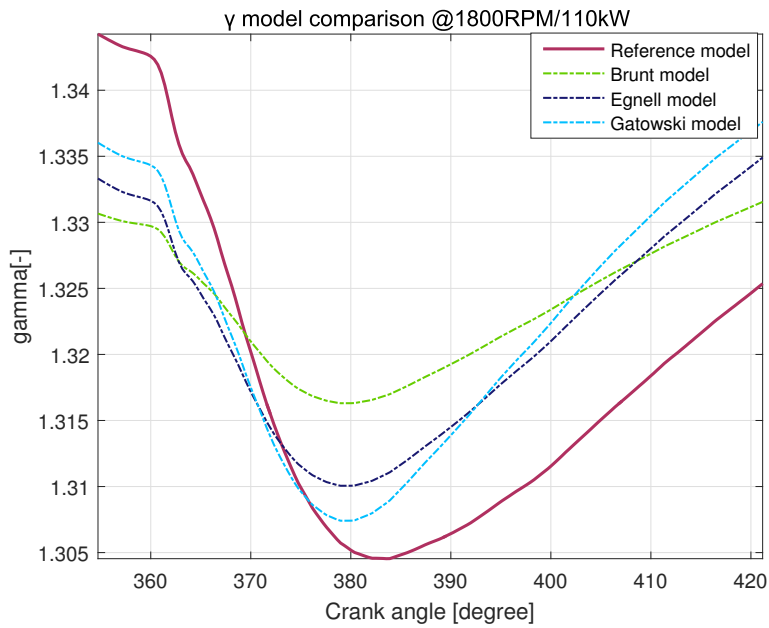
Figure A.3: Retrofit γ model candidates comparison in $E2$ cycle



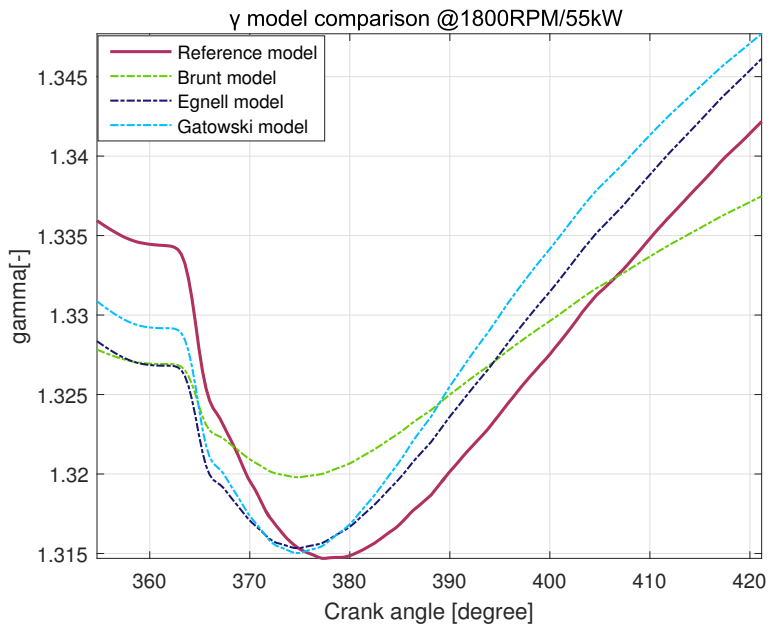
(a) 100%load / 100%speed



(b) 75%load/ 91%speed

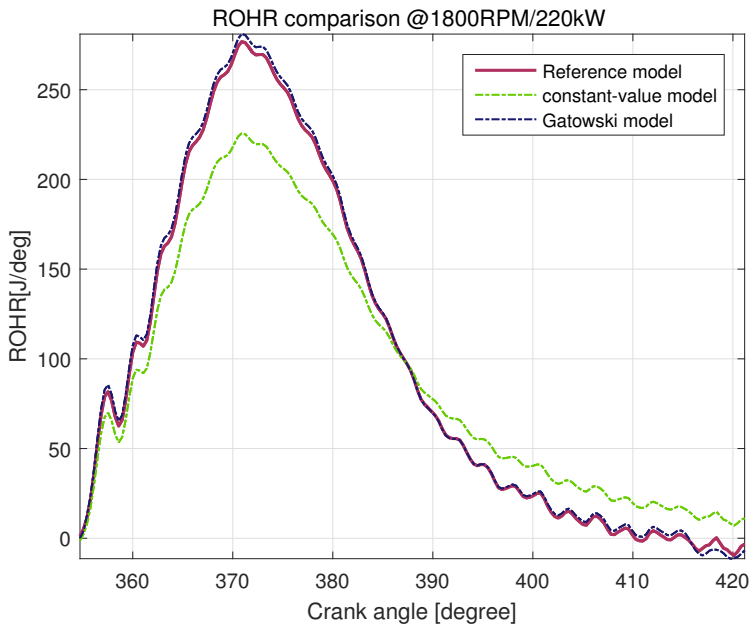


(c) 50%load/ 80%speed

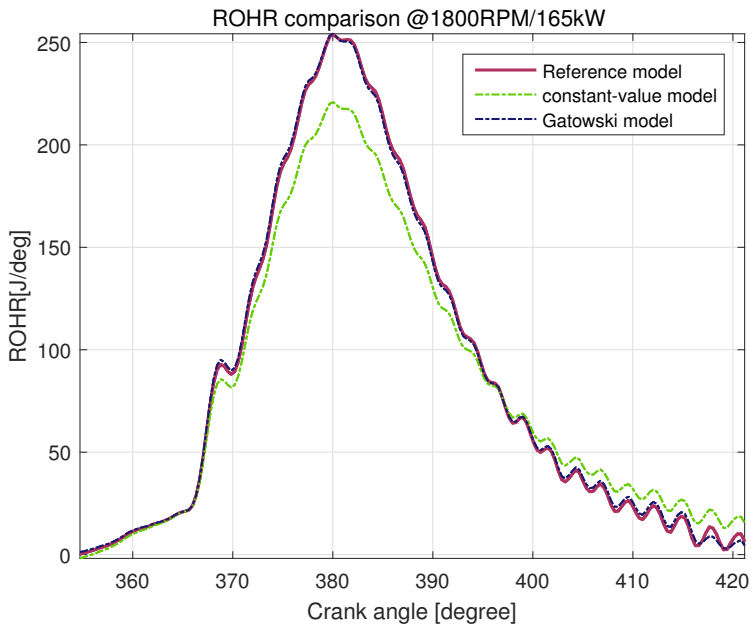


(d) 25%load/ 63%speed

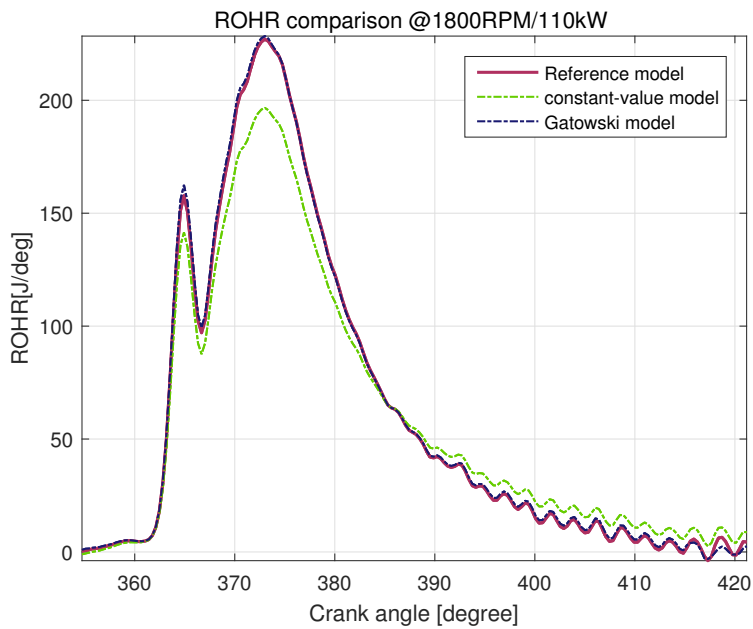
Figure A.4: Retrofit γ model candidates comparison in $E3$ cycle



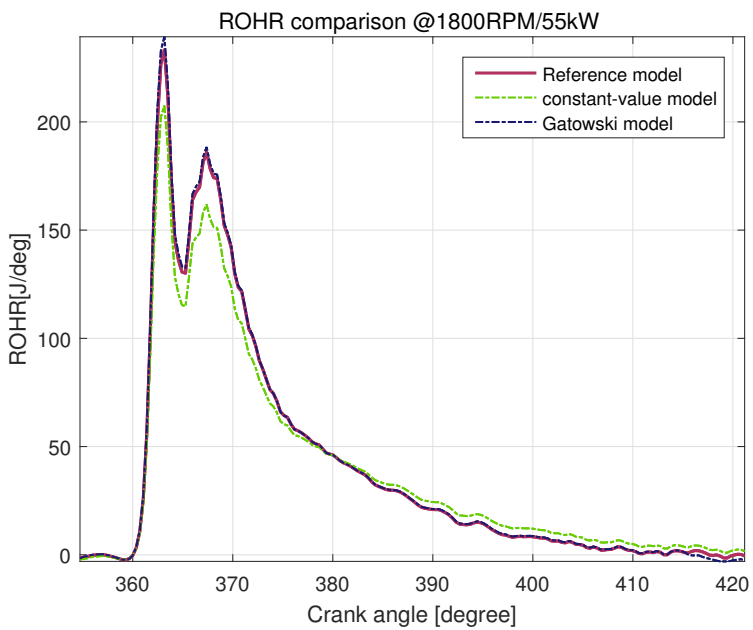
(a) 100%load / 100%speed



(b) 75%load/ 100%speed

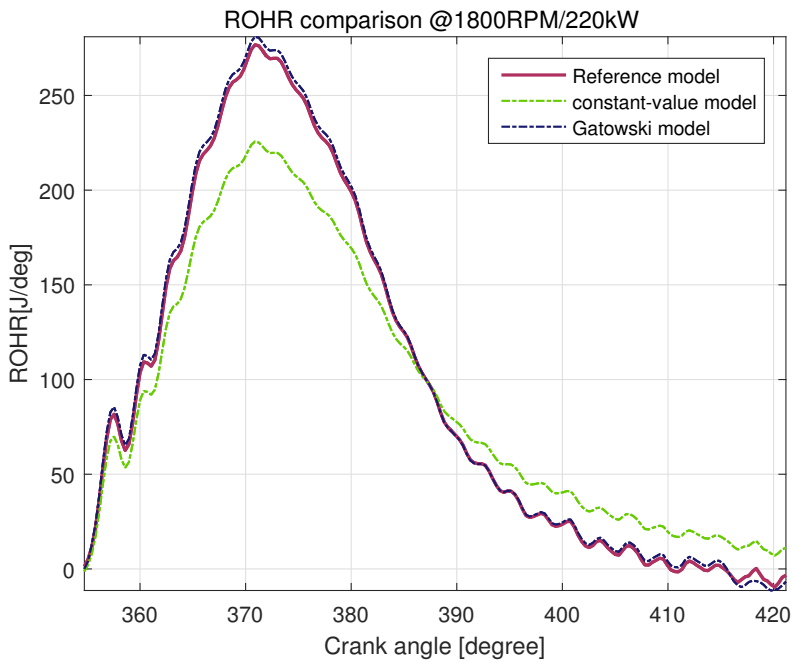


(c) 50%load/ 100%speed

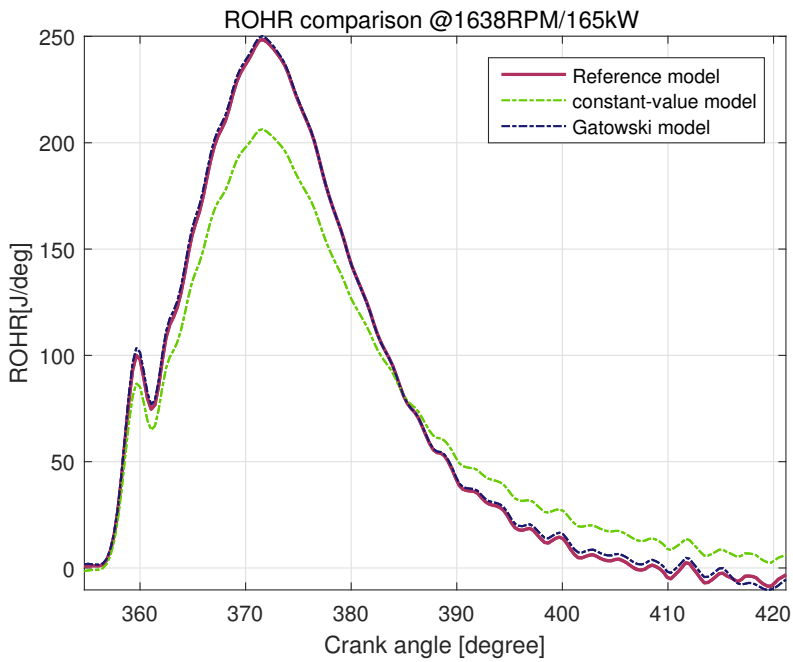


(d) 25%load/ 100%speed

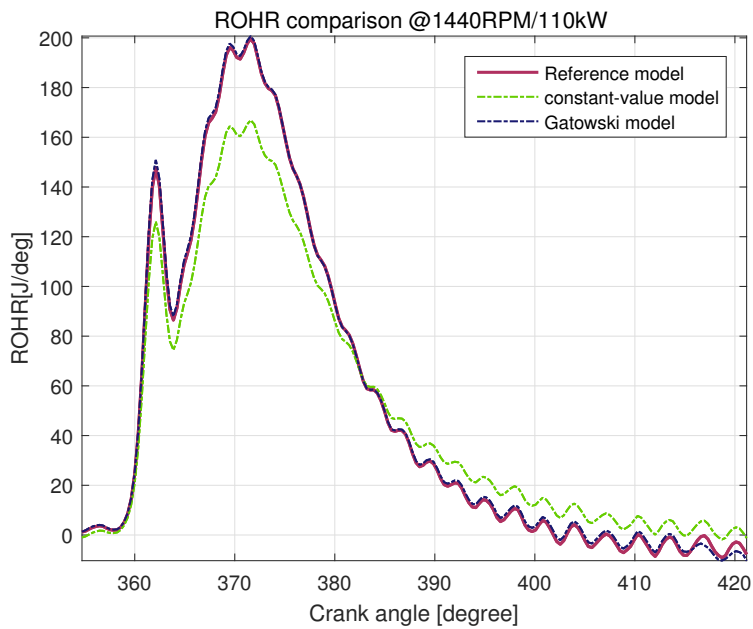
Figure A.5: The comparison of ROHR computed by retrofit γ model and constant-value γ in *E2* cycle



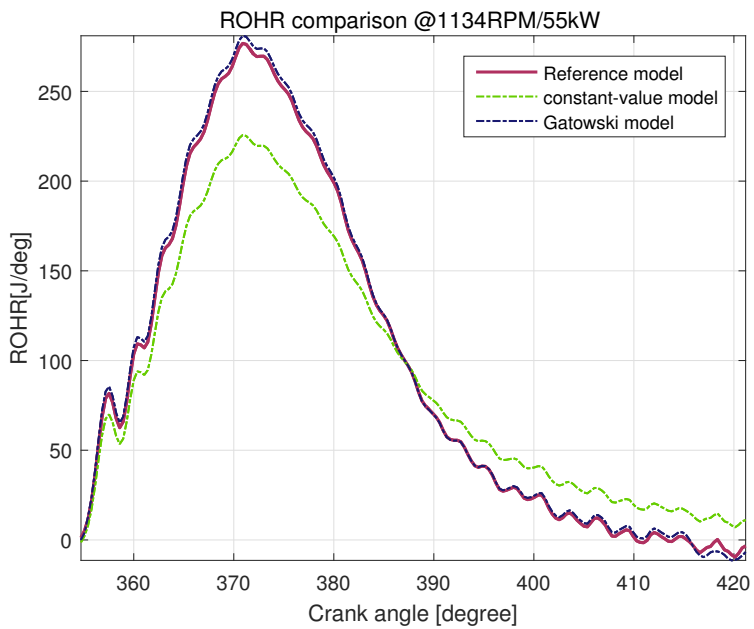
(a) 100%load / 100%speed



(b) 75%load / 91%speed



(c) 50%load/ 80%speed



(d) 25%load/ 63%speed

Figure A.6: The comparison of ROHR computed by retrofit γ model and constant-value γ in *E3* cycle

Appendix **B**

Zacharias formulas

The reference model used for evaluation of γ model candidates is built up based Zacharias formulas. This chapter depicts the basic principle of Zacharias formulas.

1. Introduction.

Zacharias [1] has developed formulas for thermodynamic properties of combustion products at chemical equilibrium formed by combustion of a pure hydrocarbon fuel C_nH_{2n} and dry air.

Zacharias carried out extensive chemical equilibrium computations for combustion products in a wide range of temperature and pressure and computed the corresponding thermodynamic properties. He then fitted a modified Beattie-Bridgeman type equation of state to his computed database and arrived at a set of three basic functions, which have become known as Zacharias formulas. The formulas are valid for lean combustion ($\lambda > 1$) in a wide range of temperature and pressure.

Later on Zacharias[2] presented a suite of computer programs which allowed evaluation of all thermodynamic properties, given almost any combination of free variables. Zacharias formulas have received wide acceptance due to their favorable accuracy and wide range of allowed temperature and pressure.

When used in simulation of dynamic processes, for example in models of internal combustion engines, the partial derivatives of the properties must be evaluated along with the properties themselves. Partial derivatives can be found by derivation of the basic functions. A subroutine for computation of the properties and their partial derivatives was developed by H.Valland [3]. The present paper contains the details of the computation in that routine.

2. The basic functions.

Zacharias non-dimensional representation of the thermodynamic property functions:

$$Z = \frac{pV}{R_0T} = Z(\theta, \pi, r) \quad \text{Compressibility function}$$

$$\phi = \frac{H}{R_0T} = \phi(\theta, \pi, r) \quad \text{Enthalpy function}$$

$$\psi = \frac{S}{R_0} = \psi(\theta, \pi, r) \quad \text{Entropy function}$$

Non-dimensional temperature θ , pressure π , and air content r are free variables in these functions:

$$\theta = T/1000 \quad T = \text{Temperature [K]}$$

$$\pi = p/0.980665 \quad p = \text{Pressure [bar]}$$

$$r = \frac{1-F}{1+f_s F} \quad F = \text{Fuel-air equivalence ratio}$$

$$f_s = \text{stoichiometric fuel-air mass ratio}$$

$$R_0 = 8314.7[J/mole] \quad \text{Universal gas constant}$$

Computation of the gas constant, specific enthalpy, and specific entropy follows:

$$R = R_0 Z$$

$$H = R_0 T \phi$$

$$S = R_0 \psi$$

The partial derivatives can be determined by derivation of the functions:

$$\frac{\partial R}{\partial T} = R_0 \frac{\partial Z}{\partial \theta} \frac{\partial \theta}{\partial T} \qquad \frac{\partial H}{\partial T} = R_0 \left(\phi + T \frac{\partial \phi}{\partial \theta} \frac{\partial \theta}{\partial T} \right) \qquad \frac{\partial S}{\partial T} = R_0 \frac{\partial \psi}{\partial \theta} \frac{\partial \theta}{\partial T}$$

$$\frac{\partial R}{\partial p} = R_0 \frac{\partial Z}{\partial \pi} \frac{\partial \pi}{\partial p} \qquad \frac{\partial H}{\partial p} = R_0 T \frac{\partial \phi}{\partial \pi} \frac{\partial \pi}{\partial p} \qquad \frac{\partial S}{\partial p} = R_0 \frac{\partial \psi}{\partial \pi} \frac{\partial \pi}{\partial p}$$

$$\frac{\partial R}{\partial F} = R_0 \frac{\partial Z}{\partial r} \frac{\partial r}{\partial F} \qquad \frac{\partial H}{\partial F} = R_0 T \frac{\partial \phi}{\partial r} \frac{\partial r}{\partial F} \qquad \frac{\partial S}{\partial F} = R_0 \frac{\partial \psi}{\partial r} \frac{\partial r}{\partial F}$$

The derivatives of the non-dimensional free variables are:

$$\frac{\partial \theta}{\partial T} = 1/1000 \qquad \frac{\partial \pi}{\partial p} = 1/0.980665 \qquad \frac{\partial r}{\partial F} = \frac{-(1 + f_s)}{(1 + f_s F)^2}$$

The computational problem has now been reduced to that of computing the basic functions (Z, ϕ, ψ) and their partial derivatives:

$$\frac{\partial Z}{\partial \theta}, \frac{\partial Z}{\partial \pi}, \frac{\partial Z}{\partial r} \qquad \frac{\partial \phi}{\partial \theta}, \frac{\partial \phi}{\partial \pi}, \frac{\partial \phi}{\partial r} \qquad \frac{\partial \psi}{\partial \theta}, \frac{\partial \psi}{\partial \pi}, \frac{\partial \psi}{\partial r}$$

Note that the above expressions are all molar quantities. Corresponding mass specific quantities can be computed using the mean molar mass of the combustion products, as shown in Chapter 6.

3. The compressibility function.

According to Zacharias the compressibility can be expressed as the sum of four terms:

$$Z = Z_0 + Z_R + Z_1 + Z_2$$

| | | |
|---------------------|---|-------------------------------------|
| The indices denote: | 0 | ideal gas contribution |
| | R | real gas correction |
| | 1 | lower stage dissociation correction |
| | 2 | upper stage dissociation correction |

3.1 Ideal gas contribution:

$$Z_0 = 1$$

$$\frac{\partial Z_0}{\partial \theta} = \frac{\partial Z_0}{\partial \pi} = \frac{\partial Z_0}{\partial r} = 0$$

3.2 The real gas correction term:

$$Z_R = \frac{\pi}{\theta} \left[B_0 - \frac{A}{\theta} e^{D/\theta^2} \right]$$

with:

$$A = 2.77105 \cdot 10^{-4} - 0.900711 \cdot 10^{-4} \cdot r$$

$$B_0 = 6.42217 \cdot 10^{-4} - 0.98367 \cdot 10^{-4} \cdot r$$

$$D = 0.8868 \cdot 10^{-2} - 0.6131 \cdot 10^{-2} \cdot r$$

$$\frac{\partial Z_R}{\partial \theta} = \frac{\pi}{\theta^2} \left[-B_0 + \frac{2A}{\theta} e^{D/\theta^2} \left(1 - \frac{D}{\theta^2} \right) \right]$$

$$\frac{\partial Z_R}{\partial \pi} = \frac{1}{\theta} \left[B_0 - \frac{A}{\theta} e^{D/\theta^2} \right]$$

$$\frac{\partial Z_R}{\partial r} = \frac{\pi}{\theta} \left[\frac{\partial B_0}{\partial r} - \frac{1}{\theta} e^{D/\theta^2} \left(\frac{\partial A}{\partial r} + \frac{A}{\theta^2} \frac{\partial D}{\partial r} \right) \right]$$

3.3 Lower stage dissociation correction:

$$Z_1 = \frac{(0.420 - 0.193 \cdot r) \pi^{+0.007}}{1 + \frac{1}{\theta} e^{y_1}} = \frac{u}{v}$$

$$u = (0.420 - 0.193 \cdot r) \pi^{+0.007}$$

$$\frac{\partial u}{\partial \theta} = 0$$

$$\frac{\partial u}{\partial \pi} = u \cdot \frac{0.007}{\pi}$$

$$\frac{\partial u}{\partial r} = -0.193 \cdot \pi^{+0.007}$$

$$v = 1 + \frac{1}{\theta} e^{y_1}$$

$$\frac{\partial v}{\partial \theta} = \frac{e^{y_1}}{\theta^2} (\theta \cdot \frac{\partial y_1}{\partial \theta} - 1)$$

$$\frac{\partial v}{\partial \pi} = \frac{1}{\theta} e^{y_1} \cdot \frac{\partial y_1}{\partial \pi}$$

$$\frac{\partial v}{\partial r} = \frac{1}{\theta} e^{y_1} \cdot \frac{\partial y_1}{\partial r}$$

Derivation of the complicated function y_1 is done by derivation of each of its individual terms:

$$y_1 = y_{11} + y_{12} + y_{13} + y_{14}$$

$$y_{11} = 15 \cdot \left(\frac{\theta}{1.65} \right)^{\left[-0.51\pi^{-0.103} - 0.14 + (0.12 - 0.29\pi^{-0.127}) \ln \frac{\theta}{1.65} \right]}$$

$$y_{12} = -6.9078$$

$$y_{13} = -\left[(1-r) - (1-r)^4 \cdot 0.2772 \right] \cdot 0.9088\pi^{-0.0212}$$

$$y_{14} = +(0.573 + 0.083 \ln \pi) \cdot e^{-0.306\theta}$$

Partial derivatives:

$$\frac{\partial y_1}{\partial \theta} = y_{11} \cdot \left\{ -0.51 \cdot \pi^{-0.103} - 0.14 + 2(0.12 - 0.29 \cdot \pi^{-0.127}) \cdot \ln \frac{\theta}{1.65} \right\} \cdot \frac{1}{\theta} - 0.306 \cdot y_{14}$$

$$\frac{\partial y_1}{\partial \pi} = y_{11} \cdot \left\{ 0.05253 \cdot \pi^{-0.103} + 0.03683 \cdot \pi^{-0.127} \cdot \ln \frac{\theta}{1.65} \right\} \cdot \frac{1}{\pi} \cdot \ln \frac{\theta}{1.65}$$

$$+ y_{13} \cdot \frac{0.0212}{\pi} + e^{-0.306\theta} \cdot \frac{0.083}{\pi}$$

$$\frac{\partial y_1}{\partial r} = (1 - 1.1088 \cdot (1-r)^3) \cdot 0.9088 \cdot \pi^{-0.0212}$$

$$\begin{aligned}\frac{\partial Z_1}{\partial \theta} &= \frac{1}{v} \left(\frac{\partial u}{\partial \theta} - Z_1 \cdot \frac{\partial v}{\partial \theta} \right) \\ \frac{\partial Z_1}{\partial \pi} &= \frac{1}{v} \left(\frac{\partial u}{\partial \pi} - Z_1 \cdot \frac{\partial v}{\partial \pi} \right) \\ \frac{\partial Z_1}{\partial r} &= \frac{1}{v} \left(\frac{\partial u}{\partial r} - Z_1 \cdot \frac{\partial v}{\partial r} \right)\end{aligned}$$

3.4 Upper level dissociation correction:

$$Z_2 = \frac{0.774 - 0.119 \cdot r - (0.0128 + 0.005r) \ln \pi}{1 + \frac{1}{\theta} e^{y_2}} = \frac{m}{n}$$

$$m = 0.774 - 0.119 \cdot r - (0.0128 + 0.005 \cdot r) \ln \pi$$

$$\frac{\partial m}{\partial \theta} = 0$$

$$\frac{\partial m}{\partial \pi} = -(0.0128 + 0.005 \cdot r) \cdot \frac{1}{\pi}$$

$$\frac{\partial m}{\partial r} = -0.119 - 0.005 \cdot \ln \pi$$

$$n = 1 + \frac{1}{\theta} e^{y_2}$$

$$\frac{\partial n}{\partial \theta} = \frac{e^{y_2}}{\theta^2} \left(\theta \cdot \frac{\partial y_2}{\partial \theta} - 1 \right)$$

$$\frac{\partial n}{\partial \pi} = \frac{e^{y_2}}{\theta} \cdot \frac{\partial y_2}{\partial \pi}$$

$$\frac{\partial n}{\partial r} = \frac{e^{y_2}}{\theta} \cdot \frac{\partial y_2}{\partial r} = 0$$

Derivation of the function y_2 is stright-forward:

$$y_2 = 18.0972 - 2.43 \cdot \theta \cdot \pi^{-0.045}$$

$$\frac{\partial y_2}{\partial \theta} = -2.43 \cdot \pi^{-0.045}$$

$$\frac{y_2}{\partial \pi} = 0.10206 \cdot \theta \cdot \pi^{-0.045} \cdot \frac{1}{\pi}$$

$$\frac{\partial y_2}{\partial r} = 0$$

$$\frac{\partial Z_2}{\partial \theta} = \frac{1}{n} \left(\frac{\partial m}{\partial \theta} - Z_2 \frac{\partial n}{\partial \theta} \right)$$

$$\frac{\partial Z_2}{\partial \pi} = \frac{1}{n} \left(\frac{\partial m}{\partial \pi} - Z_2 \frac{\partial n}{\partial \pi} \right)$$

$$\frac{\partial Z_2}{\partial r} = \frac{1}{n} \cdot \left(\frac{\partial m}{\partial r} - Z_2 \frac{\partial n}{\partial r} \right)$$

4. The enthalpy function.

The enthalpy function is expressed in a way similar to that of the compressibility:

$$\phi = \phi_0 + \phi_R + \phi_1 + \phi_2$$

4.1 The ideal gas contribution:

$$\phi_0 = \sum_{i=0}^6 a_i \theta^i$$

with

$$a_0 = +3.514956 - 0.005026 \cdot r$$

$$a_1 = +0.131438 - 0.383504 \cdot r$$

$$a_2 = +0.477182 + 0.185214 \cdot r$$

$$a_3 = -0.287367 - 0.694862 \cdot 10^{-1} \cdot r$$

$$a_4 = +0.742561 \cdot 10^{-1} + 0.164041 \cdot 10^{-1} \cdot r$$

$$a_5 = -0.916344 \cdot 10^{-2} - 0.204537 \cdot 10^{-2} \cdot r$$

$$a_6 = +0.439896 \cdot 10^{-3} + 0.101610 \cdot 10^{-3} \cdot r$$

$$\frac{\partial \phi_0}{\partial \theta} = \sum_{i=1}^6 a_i \cdot i \cdot \theta^{i-1}$$

$$\frac{\partial \theta_0}{\partial \pi} = 0$$

$$\frac{\partial \phi_0}{\partial r} = \sum_{i=0}^6 \frac{\partial a_i}{\partial r} \cdot \theta^i$$

4.2 The real gas correction term:

$$\phi_R = \frac{\pi}{\theta} \left[B_0 - \frac{2A}{\theta} e^{D/\theta^2} \left(1 + \frac{D}{\theta^2} \right) \right]$$

$$\frac{\partial \phi_R}{\partial \theta} = \frac{\pi}{\theta^2} \left[-B_0 + \frac{4A}{\theta} e^{D/\theta^2} \left\{ \left(1 + \frac{D}{\theta^3} \right) \left(1 + \frac{D}{\theta^2} \right) + \frac{D}{\theta^3} \right\} \right]$$

$$\frac{\partial \phi_R}{\partial \pi} = \frac{1}{\theta} \left[B_0 - \frac{2A}{\theta} e^{D/\theta^2} \left(1 + \frac{D}{\theta^2} \right) \right]$$

$$\frac{\partial \phi_R}{\partial r} = \frac{\pi}{\theta} \left[\frac{\partial B_0}{\partial r} - \frac{2}{\theta} e^{D/\theta^2} \left\{ \frac{\partial A}{\partial r} \left(1 + \frac{D}{\theta^2} \right) + \frac{2A}{\theta^2} \frac{\partial D}{\partial r} \right\} \right]$$

4.3 Lower stage dissociation correction:

$$\phi_1 = \frac{(25.9 - 11.0r)\pi^{+0.0115}}{\theta\left(1 + \frac{1}{\theta}e^{y_1}\right)} = \frac{q}{t}$$

$$q = (25.9 - 11.0r)\pi^{+0.0115}$$

$$\frac{\partial q}{\partial \theta} = 0$$

$$\frac{\partial q}{\partial \pi} = q \cdot \frac{0.0115}{\pi}$$

$$\frac{\partial q}{\partial r} = -11.0 \cdot \pi^{+0.0115}$$

$$t = \theta\left(1 + \frac{1}{\theta}e^{y_1}\right)$$

$$\frac{\partial t}{\partial \theta} = 1 + e^{y_1} \cdot \frac{\partial y_1}{\partial \theta}$$

$$\frac{\partial t}{\partial \pi} = e^{y_1} \cdot \frac{\partial y_1}{\partial \pi}$$

$$\frac{\partial t}{\partial r} = e^{y_1} \cdot \frac{\partial y_1}{\partial r}$$

$$\frac{\partial \phi_1}{\partial \theta} = \frac{1}{t} \left[-\phi_1 \cdot \frac{\partial t}{\partial \theta} \right]$$

$$\frac{\partial \phi_1}{\partial \pi} = \frac{1}{t} \left[\frac{\partial q}{\partial \pi} - \phi_1 \cdot \frac{\partial t}{\partial \pi} \right]$$

$$\frac{\partial \phi_1}{\partial r} = \frac{1}{t} \left[\frac{\partial q}{\partial r} - \phi_1 \cdot \frac{\partial t}{\partial r} \right]$$

4.4 Upper stage dissociation correction:

$$\phi_2 = \frac{86.50 - 3.065 \ln \pi - 14.35r}{\theta\left(1 + \frac{1}{\theta}e^{y_2}\right)} = \frac{q}{t}$$

$$q = 86.50 - 3.065 \ln \pi - 14.35r$$

$$\frac{\partial q}{\partial \theta} = 0$$

$$\frac{\partial q}{\partial \pi} = -3.065 \cdot \frac{1}{\pi}$$

$$\frac{\partial q}{\partial r} = -14.35$$

$$t = \theta \left(1 + \frac{1}{\theta} e^{y_2} \right)$$

$$\frac{\partial t}{\partial \theta} = 1 + e^{y_2} \cdot \frac{\partial y_2}{\partial \theta}$$

$$\frac{\partial t}{\partial \pi} = e^{y_2} \cdot \frac{\partial y_2}{\partial \pi}$$

$$\frac{\partial t}{\partial r} = e^{y_2} \cdot \frac{\partial y_2}{\partial r} = 0$$

$$\frac{\partial \phi_2}{\partial \theta} = \frac{1}{t} \left[-\phi_2 \cdot \frac{\partial t}{\partial \theta} \right]$$

$$\frac{\partial \phi_2}{\partial \pi} = \frac{1}{t} \left[\frac{\partial q}{\partial \pi} - \phi_2 \cdot \frac{\partial t}{\partial \pi} \right]$$

$$\frac{\partial \phi_2}{\partial r} = \frac{1}{t} \left[\frac{\partial q}{\partial r} \right]$$

5. The entropy function.

The entropy function according to Zacharias:

$$\psi = \psi_0 + \psi_R + \psi_1 + \psi_2$$

5.1 The ideal gas contribution:

$$\psi_0 = (3.5566 - 0.0659r) \ln 1000\theta + \sum_{j=0}^6 b_j \theta^j - \ln \pi - \sum_{k=0}^3 c_k r^k$$

with:

$$b_0 = +2.972979 + 0.553140 \cdot r$$

$$b_1 = +0.583837 \cdot 10^{-1} - 0.485001 \cdot r$$

$$b_2 = +0.871349 + 0.698183 \cdot 10^{-1} \cdot r$$

$$b_3 = -0.451556 - 0.287720 \cdot 10^{-2} \cdot r$$

$$b_4 = +0.109164 - 0.693663 \cdot 10^{-3} \cdot r$$

$$b_5 = -0.129754 \cdot 10^{-1} + 0.920231 \cdot 10^{-4} \cdot r$$

$$b_6 = +0.608234 \cdot 10^{-3} - 0.299679 \cdot 10^{-5} \cdot r$$

$$c_0 = -0.805214$$

$$c_1 = -0.400981$$

$$c_2 = +0.576989$$

$$c_3 = +0.060056$$

$$\frac{\partial \psi_0}{\partial \theta} = (3.5566 - 0.0659r) \cdot \frac{1}{\theta} + \sum_{j=1}^6 j b_j \theta^{j-1}$$

$$\frac{\partial \psi_0}{\partial \pi} = -\frac{1}{\pi}$$

$$\frac{\partial \psi_0}{\partial r} = -0.0659 \cdot \ln(1000 \cdot \theta) + \sum_{j=0}^6 \frac{\partial b_j}{\partial r} \theta^j - \sum_{k=1}^3 k \cdot c_k \cdot r^{k-1}$$

5.2 The real gas correction term:

$$\psi_R = \frac{\pi}{\theta} \left[-\frac{A}{\theta} e^{D/\theta^2} \left(1 + \frac{D}{\theta^2} \right) \right]$$

$$\frac{\partial \psi_R}{\partial \theta} = \frac{\pi}{\theta} \cdot \frac{A}{\theta^2} \cdot e^{D/\theta^2} \cdot 2 \left[\left(1 + \frac{D}{\theta^2} \right)^2 + \frac{D}{\theta^2} \right]$$

$$\frac{\partial \psi_R}{\partial \pi} = \psi_R \cdot \frac{1}{\pi}$$

$$\frac{\partial \psi_R}{\partial r} = -\frac{\pi}{\theta^2} \cdot e^{D/\theta^2} \cdot \left[\frac{\partial A}{\partial r} \left(1 + \frac{D}{\theta^2}\right) + \frac{A}{\theta^2} \frac{\partial D}{\partial r} \left(2 + \frac{D}{\theta^2}\right) \right]$$

5.3 Lower stage dissociation correction:

$$\psi_1 = \frac{(8.179 - 3.726r)\pi^{-0.03453}}{\left(1 + \frac{1}{\theta} e^{y_1}\right)} = \frac{u}{v}$$

$$u = (8.179 - 3.726r)\pi^{-0.03453}$$

$$\frac{\partial u}{\partial \theta} = 0$$

$$\frac{\partial u}{\partial \pi} = u \cdot (-0.03453) \cdot \frac{1}{\pi}$$

$$\frac{\partial u}{\partial r} = -3.726 \cdot \pi^{-0.03453}$$

$$v = \left(1 + \frac{1}{\theta} e^{y_1}\right)$$

$$\frac{\partial v}{\partial \theta} = \frac{1}{\theta^2} \cdot e^{y_1} \left(\theta \cdot \frac{\partial y_1}{\partial \theta} - 1\right)$$

$$\frac{\partial v}{\partial \pi} = \frac{1}{\theta} \cdot e^{y_1} \frac{\partial y_1}{\partial \pi}$$

$$\frac{\partial v}{\partial r} = \frac{1}{\theta} \cdot e^{y_1} \frac{\partial y_1}{\partial r}$$

$$\frac{\partial \psi_1}{\partial \theta} = \frac{1}{v} \left(-\psi_1 \cdot \frac{\partial v}{\partial \theta}\right)$$

$$\frac{\partial \psi_1}{\partial \pi} = \frac{1}{v} \left(\frac{\partial u}{\partial \pi} - \psi_1 \cdot \frac{\partial v}{\partial \pi}\right)$$

$$\frac{\partial \psi_1}{\partial r} = \frac{1}{v} \left(\frac{\partial u}{\partial r} - \psi_1 \cdot \frac{\partial v}{\partial r}\right)$$

5.4 Upper stage dissociation correction:

$$\psi_2 = \frac{14.512\pi^{-0.05648} - 2.434r}{\left(1 + \frac{1}{\theta} e^{y_2}\right)} = \frac{u}{v}$$

$$u = 14.512 \cdot \pi^{-0.05648} - 2.434 \cdot r$$

$$\frac{\partial u}{\partial \theta} = 0$$

$$\frac{\partial u}{\partial \pi} = 14.512 \cdot (-0.05648) \cdot \pi^{-0.05648} \cdot \frac{1}{\pi} = -0.81963776 \cdot \pi^{-0.05648} \cdot \frac{1}{\pi}$$

$$\frac{\partial u}{\partial r} = -2.434$$

$$v = \left(1 + \frac{1}{\theta} e^{y_2}\right)$$

$$\frac{\partial v}{\partial \theta} = \frac{1}{\theta^2} \cdot e^{y_2} \left(\theta \cdot \frac{\partial y_2}{\partial \theta} - 1\right)$$

$$\frac{\partial v}{\partial \pi} = \frac{1}{\theta} \cdot e^{y_2} \frac{\partial y_2}{\partial \pi}$$

$$\frac{\partial v}{\partial r} = \frac{1}{\theta} \cdot e^{y_2} \frac{\partial y_2}{\partial r} = 0$$

$$\frac{\partial \psi_2}{\partial \theta} = \frac{1}{v} \left(-\psi_2 \cdot \frac{\partial v}{\partial \theta}\right)$$

$$\frac{\partial \psi_2}{\partial \pi} = \frac{1}{v} \left(\frac{\partial u}{\partial \pi} - \psi_2 \cdot \frac{\partial v}{\partial \pi}\right)$$

$$\frac{\partial \psi_2}{\partial r} = \frac{1}{v} \left(\frac{\partial u}{\partial r}\right)$$

6. Mass specific properties.

The basic functions allow computation of specific properties on a molar basis.

In many applications mass specific quantities are more convenient. Mass specific quantities can be computed using the mean molecular mass of the combustion products. Although Zacharias has computed the equilibrium composition of the products, he does not present any function for the mean molecular mass.

Assuming complete combustion with access air, it can be shown [4] that the mean molar mass is a function of the fuel-air equivalence ratio:

$$M = M(F)$$

Assuming the composition of the dry air as:

| | |
|----------------|-------------|
| Oxygen | 1.0000 mole |
| Nitrogen | 3.7274 mole |
| Argon | 0.0444 mole |
| Carbon dioxide | 0.0014 mole |

Using the following molar masses:

| | | |
|----------------|------------------|--------|
| Oxygen | O ₂ | 31.999 |
| Water | H ₂ O | 18.016 |
| Carbon dioxide | CO ₂ | 44.010 |
| Nitrogen | N ₂ | 28.013 |
| Argon | Ar | 39.948 |

We arrive at the following expression for the mean molecular mass of the products, and its partial derivative with respect to F :

$$M = \frac{138.2500 + 9.3517 \cdot F}{4.7732 + 0.333333 \cdot F} \qquad \frac{\partial M}{\partial F} = \frac{-1.44575}{(4.7732 + 0.333333 \cdot F)^2}$$

In this case the mass specific quantities can be evaluated:

$$\begin{aligned} R_m &= \frac{R}{M} & h &= \frac{H}{M} & s &= \frac{S}{M} \\ \frac{\partial R_m}{\partial T} &= \frac{1}{M} \frac{\partial R}{\partial T} & \frac{\partial h}{\partial T} &= \frac{1}{M} \frac{\partial H}{\partial T} & \frac{\partial s}{\partial T} &= \frac{1}{M} \frac{\partial S}{\partial T} \\ \frac{\partial R_m}{\partial p} &= \frac{1}{M} \frac{\partial R}{\partial p} & \frac{\partial h}{\partial p} &= \frac{1}{M} \frac{\partial H}{\partial p} & \frac{\partial s}{\partial p} &= \frac{1}{M} \frac{\partial S}{\partial p} \\ \frac{\partial R_m}{\partial F} &= \frac{1}{M} \left(\frac{\partial R}{\partial F} - R_m \frac{\partial M}{\partial F} \right) & \frac{\partial h}{\partial F} &= \frac{1}{M} \left(\frac{\partial H}{\partial F} - h \frac{\partial M}{\partial F} \right) & \frac{\partial s}{\partial F} &= \frac{1}{M} \left(\frac{\partial S}{\partial F} - s \frac{\partial M}{\partial F} \right) \end{aligned}$$

Other thermodynamic properties may be derived from those computed directly using the basic functions:

Specific internal energy:

$$u = h - RT$$

Specific heat capacity at constant pressure:

$$c_p = \left(\frac{\partial h}{\partial T} \right)_p$$

$$c_v = \left(\frac{\partial u}{\partial T} \right)_p + \left(\frac{\partial u}{\partial p} \right)_T \cdot \frac{\frac{R}{p} + \frac{\partial R}{\partial T}}{\frac{R}{p} - \frac{\partial R}{\partial p}}$$

Adiabatic exponent:

$$\kappa = c_p / c_v$$

Specific Gibbs free enthalpy:

$$g = h - Ts$$

Specific Helmholtz free energy:

$$a = u - Ts$$

7. Consistency-test of the formulas.

The Zacharias formulas have many terms, each with a complex structure. There are many possibilities for introducing errors when deriving formulas for other properties and their derivatives. Verification is therefore a must, and should be done with greatest care.

Zacharias did not supply any test values for his formulas. We therefore have to apply some other approach. One such possibility is to employ the Maxwell relations. When temperature T and pressure p are free variables the following relations lend themselves for such verification:

$$\left(\frac{\partial g}{\partial T} \right)_p = -s \qquad \left(\frac{\partial g}{\partial p} \right)_T = v \qquad \left(\frac{\partial s}{\partial p} \right)_T = - \left(\frac{\partial v}{\partial T} \right)_p$$

For each relation, the left-hand side and the right hand side should be computed individually and compared. Ideally the difference should be zero, but small deviations indicates consistency of the formulas.

Consistency tests of this type have proved that the mass specific properties derived from Zacharias formulas are valid at states where dissociation is negligible, i.e. temperatures below approximately 1700 K.

8. Implementation in computer programs.

The computation of mass specific properties has been implemented in a set of Fortran subroutines. All routines take (p,T,F) as input values and compute various output properties. The calling sequence and explanation of the formal parameters follows below.

subroutine zach1(p,T,F,DCO,R,u,h,s,k,up,uT,uF,Rp,RT,RF)

The routine computes the adiabatic exponent and partial derivatives of u and R. Partial derivatives are required in certain dynamic process models. This routine is compatible with the original subroutine called GASDTA.

subroutine zach2(p,T,F,DCO,u,h,s,R,k,cv,cp)

The routine has no partial derivatives as output variables, but specific heats and the adiabatic exponent is computed.

subroutine zach3(p,T,F,DCO,h,u,s,hp,hT,hF,up,uT,uF,sp,sT,sF,Rp,RT,RF,R,cp,cv,k)

The routine is an extension of zach1 and zach2. Partial derivatives are computed for (h, u, s, and R).

Input parameters:

| | |
|---------|--|
| p | pressure [Pa] |
| T | temperature [K] |
| F | fuel air equivalence ratio [-] ($F = 1/\lambda$) |
| DCO | control parameter: |
| DCO = 0 | ideal gas properties with real gas correction |
| DCO = 1 | correction for lower stage dissociation added |
| DCO = 2 | correction for upper stage dissociation added |

Output parameters:

| | |
|----------|---|
| h | specific enthalpy [J/kg] |
| u | specific internal energy [J/kg] |
| s | specific entropy [J/kgK] |
| hp,hT,hF | partial derivatives of h with respect to p,T,F. |
| up,uT,uF | partial derivatives of u with respect to p,T,F. |
| sp,sT,sF | partial derivatives of s with respect to p,T,F. |
| Rp,RT,RF | partial derivatives of R with respect to p,T,F. |
| R | gas constant [J/kgK] |
| cp | specific heat at constant pressure [J/kgK] |
| cv | specific heat at constant volume [J/kgK] |
| k | ratio of specific heats: $k=cp/cv$ |